

Performance Model
of Gas Turbine Combined Cycle Systems

Prepared by:

H. Christopher Frey
Yunhua Zhu
Department of Civil, Construction, and Environmental Engineering
North Carolina State University
Raleigh, NC

Prepared for:

Center for Energy and Environmental Studies
Carnegie Mellon University
Pittsburgh, PA

October 20, 2004

Table of Contents

1.0	INTRODUCTION.....	1
2.0	SIMPLE CYCLE GAS TURBINE MASS AND ENERGY BALANCE MODEL	2
2.1	COMPRESSOR	4
2.2	COMBUSTOR	8
2.3	TURBINE	14
2.4	NET POWER OUTPUT.....	19
3.0	COMBINED CYCLE GAS TURBINE MASS AND ENERGY BALANCE	23
4.0	CALIBRATION OF THE PERFORMANCE MODEL	26
4.1	NATURAL GAS	26
4.2	SYNGAS	29
4.3	DISCUSSION OF CALIBRATION RESULTS.....	34
5.0	COST MODEL.....	35
5.1	NATURAL GAS COMBINED CYCLE	36
5.2	SYNGAS-FUELED GAS TURBINE.....	39
6.0	SENSITIVITY ANALYSIS OF DIFFERENT SYNGAS COMPOSITIONS AND INPUTS.....	41
6.1	EFFECTS OF MOISTURE FRACTION AND CO ₂ REMOVAL.....	41
	<i>6.1.1 Effects of Moisture Fraction</i>	<i>44</i>
	<i>6.1.2 Effects of CO₂ Removal.....</i>	<i>45</i>
6.2	EFFECTS OF DIFFERENT PUBLISHED SYNGAS COMPOSITIONS	47
7.0	SENSITIVITY OF INPUTS	50
8.0	DISCUSSION OF SENSITIVITY ANALYSIS	53
9.0	CONCLUSIONS	55
10.0	NOMENCLATURE.....	57
11.0	REFERENCES.....	60

List of Tables

Figure 1. Simplified Schematic Diagram of a Simple Cycle Gas Turbine.....	2
Figure 2. Simplified Diagram of a Three-Stage Compressor.....	4
Figure 3. Regression Results for Entropy as a Function of Temperature for Air.....	6
Figure 4. Regression Results for Temperature as a Function of Entropy for Air.....	6
Figure 5. Regression Results for Enthalpy as a Function of Temperature for Air.....	8
Figure 6. Regression Results for Temperature as a Function of Enthalpy for Air.....	8
Figure 7. Simplified Diagram of a Three-Stage Turbine.....	14
Figure 8. Regression Results for Entropy as a Function of Temperature for Nitrogen (N ₂).....	17
Figure 9. Regression Results for Temperature as a Function of Entropy for Nitrogen (N ₂).....	17
Figure 10. Regression Results for Enthalpy as a Function of Temperature for Nitrogen (N ₂)....	17
Figure 11. Regression Results for Temperature as a Function of Enthalpy for Nitrogen (N ₂)....	18
Figure 12. Calibration of the Gas Turbine Model – plots of (a) Exhaust Temperature, (b) Simple Cycle Efficiency, and (c) Simple Cycle Output versus Adiabatic Compressor Efficiency of Gas Turbine.	28
Figure 13. Calibration of the Gas Turbine Model – plots of (a) Exhaust Temperature, (b) Simple Cycle Efficiency, and (c) Simple Cycle Output versus Adiabatic Compressor Efficiency of Gas Turbine.	33
Figure 14. Changes in Inputs versus Changes in Gas Turbine (GT) Power Output.....	51
Figure 15. Changes in Inputs versus Changes in Simple Cycle Efficiency.....	52
Figure 16. Changes in Inputs versus Changes in Combined Cycle Efficiency.....	52

List of Figures

Figure 1. Simplified Schematic Diagram of a Simple Cycle Gas Turbine.....	2
Figure 2. Simplified Diagram of a Three-Stage Compressor	4
Figure 3. Regression Results for Entropy as a Function of Temperature for Air.....	6
Figure 4. Regression Results for Temperature as a Function of Entropy for Air.....	6
Figure 5. Regression Results for Enthalpy as a Function of Temperature for Air	8
Figure 6. Regression Results for Temperature as a Function of Enthalpy for Air	8
Figure 7. Simplified Diagram of a Three-Stage Turbine.....	14
Figure 8. Regression Results for Entropy as a Function of Temperature for Nitrogen (N ₂)	17
Figure 9. Regression Results for Temperature as a Function of Entropy for Nitrogen (N ₂).....	17
Figure 10. Regression Results for Enthalpy as a Function of Temperature for Nitrogen (N ₂)....	17
Figure 11. Regression Results for Temperature as a Function of Enthalpy for Nitrogen (N ₂)....	18
Figure 12. Calibration of the Gas Turbine Model – plots of (a) Exhaust Temperature, (b) Simple Cycle Efficiency, and (c) Simple Cycle Output versus Adiabatic Compressor Efficiency of Gas Turbine.	28
Figure 13. Calibration of the Gas Turbine Model – plots of (a) Exhaust Temperature, (b) Simple Cycle Efficiency, and (c) Simple Cycle Output versus Adiabatic Compressor Efficiency of Gas Turbine.	33
Figure 14. Changes in Inputs versus Changes in Gas Turbine (GT) Power Output.....	51
Figure 15. Changes in Inputs versus Changes in Simple Cycle Efficiency.....	52
Figure 16. Changes in Inputs versus Changes in Combined Cycle Efficiency	52

1.0 Introduction

The purpose of this report is to document a performance model for gas turbine combined cycle systems. The model is intended for incorporation into the Integrated Environmental Control Model (IECM), which has been developed by Carnegie Mellon University (CMU) under sponsorship of the U.S. Department of Energy (e.g., Rubin *et al.*, 1986, 1988, 1991, 1997; Berkenpas *et al.*, 1999). Under subcontract to CMU, North Carolina State University has developed the performance model for gas turbine combined cycle systems. The performance model for the IECM builds upon experience from development of process simulation models of gas turbine systems in ASPEN (e.g., Frey and Rubin, 1990; Frey and Akunuri, 2001).

Gas turbines have been widely used for power generation. A typical simple cycle, natural gas-fired turbine can obtain an efficiency of 35% or greater (Brooks, 2000). Most new power plants also use a heat recovery steam generator (HRSG) and steam turbine in addition to a gas turbine. When used together, gas and steam turbines constitute a combined cycle system. In a combined cycle system, the waste heat in the exhaust gas is recovered to generate high temperature steam for a steam turbine.

The objective of this study was to develop a performance model of simple and combined cycle gas turbine power plants. The mass and energy balance models for simple cycle and combined cycle plants were implemented in an Excel spreadsheet. The method for calibrating the models is discussed and illustrated with examples based on natural gas and syngas.

The next section focuses on documentation of the performance model for a simple cycle gas turbine. Section 3.0 documents the performance model for a combined cycle system. The procedure for calibration of the gas turbine combined cycle model for both natural gas and syngas is demonstrated in Section 4.

2.0 Simple Cycle Gas Turbine Mass and Energy Balance Model

The simple cycle gas turbine (SCGT) mass and energy balance model is based upon the air-standard Brayton cycle, as described in Wark (1983). The case study examples are based upon data reported by General Electric for the Frame 7F gas turbine design (Brooks, 2000).

A SCGT is comprised of three major components, including the compressor, combustor, and turbine, as shown in Figure 1. Air, at ambient pressure, P_a , and ambient temperature, T_a , enters the compressor. The ratio of the compressor exit pressure to the inlet ambient air pressure is defined as the pressure ratio, r_p . Compression takes place approximately adiabatically. Therefore, the temperature of the compressed air is higher than the ambient temperature of the inlet air. The performance of an ideal adiabatic and isentropic compressor can be calculated using straight-forward thermodynamic principles. However, because real compressors are subject to inefficiencies, their performance will not be as good as the ideal case. Therefore, adiabatic compressor efficiency, η_c , is defined to more accurately represent the real world performance of a compressor.

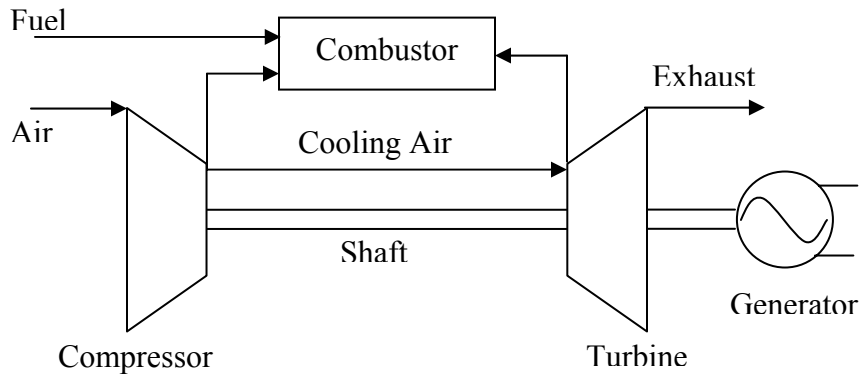


Figure 1. Simplified Schematic Diagram of a Simple Cycle Gas Turbine

The compressed air enters the combustor, where it is mixed with high pressure gaseous fuel. The fuel and air are burned at essentially constant pressure. The conventional fuel for SCGT systems is natural gas, which is comprised mostly of methane. However, other fuels may be burned in a gas turbine, including syngas obtained from a gasification process. Syngas typically contains carbon monoxide (CO), hydrogen (H₂), methane (CH₄), carbon dioxide (CO₂),

nitrogen (N_2), and water vapor (H_2O) as the primary constituents. Syngases also may contain relatively small amounts of hydrogen sulfide (H_2S), carbonyl sulfide (COS), and ammonia (NH_3). These latter three components are significant in terms of the formation of SO_2 and NO_x emissions, but are less important in terms of calculating the mass and energy balance of the system because they comprise only a small portion of the total fuel flow rate and the total fuel heating value. The combustor typically has a small pressure drop. Therefore, the exit pressure from the combustor is slightly less than that compared to the compressor outlet.

The high pressure, hot product gases from the combustor enter the turbine, or expander, portion of the SCGT system. In the turbine, the gases are reduced in pressure, resulting in a corresponding reduction in temperature. The heat-removal process associated with expansion and cooling of the hot gases in the turbine results in an energy transfer from the gases to shaft work, leading to rotation of a shaft. In many heavy duty SCGT designs, the compressor, turbine, and generator turn on the same shaft. The turbine must supply enough rotational shaft energy to power the compressor. The net difference between the work output of the turbine and the work input to the compressor is available for producing electricity in the generator. The ratio of compressor work to turbine work is referred to as the back work ratio. The turbine inlet temperature is carefully controlled to prevent damage or fatigue of the first stage stator and rotor blades. The turbine inlet temperature and the pressure ratio are the two most important parameters that impact system efficiency.

As noted by Frey and Rubin (1991), the mass flow through a gas turbine is limited by the critical area of the turbine inlet nozzle. The critical area of the turbine inlet nozzle is a constant for a given make and model of gas turbine. Gas turbine operation on natural gas typically involves a relatively small fuel mass flow rate compared to the compressor mass flow rate. However, when operating on syngas, which may have a heating value substantially smaller than that of natural gas, a larger fuel mass flow rate is needed in order to supply approximately the same amount of energy to the gas turbine. The mass fuel-to-air ratio will be larger for a low BTU fuel than for a high BTU fuel. However, the total mass flow at the turbine inlet remains approximately the same. Therefore, the mass flow at the compressor inlet must be reduced to compensate for the higher fuel-to-air ratios needed for low BTU syngases.

The mass flow at the turbine inlet nozzle is estimated, assuming choked flow conditions, based upon the following relationship (Frey and Rubin, 1991):

$$m_{act} = m_{ref} \left(\frac{P_{act}}{P_{ref}} \right) \sqrt{\left(\frac{MW_{act}}{MW_{ref}} \right) \left(\frac{T_{ref}}{T_{act}} \right)} \quad (1)$$

The reference values are determined based upon calibration with published data for gas turbine operation on natural gas. The actual values are determined based upon the desired simulated conditions. The pressure, temperature, and molecular weight in Equation (1) are evaluated at the turbine inlet nozzle as described in Section 2.3.

The mass and energy balance for each of the following components are presented in the following sections: (1) compressor; (2) combustor; (3) turbine; and (4) net power output. The calculation of overall SCGT performance is also discussed.

2.1 Compressor

The compressor consists of three stages. From each stage, a fraction of air is extracted for use in cooling various stages of the turbine.

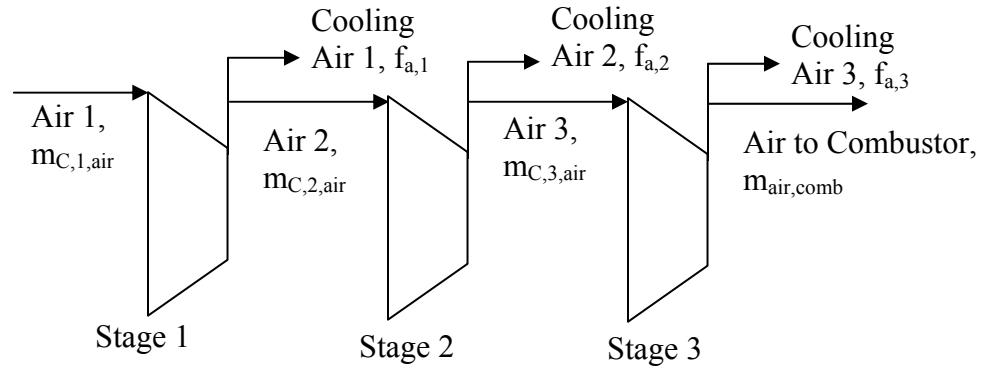


Figure 2. Simplified Diagram of a Three-Stage Compressor

The outlet pressure of a compressor is specified by multiplying the pressure ratio and the inlet pressure:

$$P_{C,out} = P_{C,in} r_p \quad (2)$$

The pressure ratio for each stage ($i=1$ to 3) is estimated as:

$$r_{p,i} = (r_p)^{0.33} \quad (3)$$

The outlet pressures for the first, second, and third stage are estimated by the following:

$$P_{C,1, out} = P_{C,in} (r_p)^{0.33} \quad (4)$$

$$P_{C,2, out} = P_{C,in} (r_p)^{0.67} \quad (5)$$

$$P_{C,3, out} = P_{C,in} r_p \quad (6)$$

The cooling air fractions split from three stages are specified as $f_{a,1}$, $f_{a,2}$, and $f_{a,3}$ of the total air flow rate, respectively. Therefore, the air flow rates through three stages and the combustor are:

$$m_{C,1,air} = m_{air} \quad (7)$$

$$m_{C,2,air} = (1 - f_{a,1}) m_{air} \quad (8)$$

$$m_{C,3,air} = (1 - f_{a,1} - f_{a,2}) m_{air} \quad (9)$$

$$m_{comb,air} = (1 - f_{a,1} - f_{a,2} - f_{a,3}) m_{air} \quad (10)$$

For each stage, the outlet temperature is estimated via a multi-step procedure. The first step is to estimate the entropy of the inlet air based upon a regression relationship of thermodynamic data as given in Figure 3:

$$s_{C,i,in} = 1.0327 \ln(T) - 4.1905 \quad (11)$$

Based upon the estimated entropy of the inlet air and the pressure ratio, the entropy of the compressor outlet air is estimated:

$$s_{C,i,out} = s_{C,i,in} + \left(\frac{R}{MW_{air}} \right) \ln(r_{p,i}) \quad (12)$$

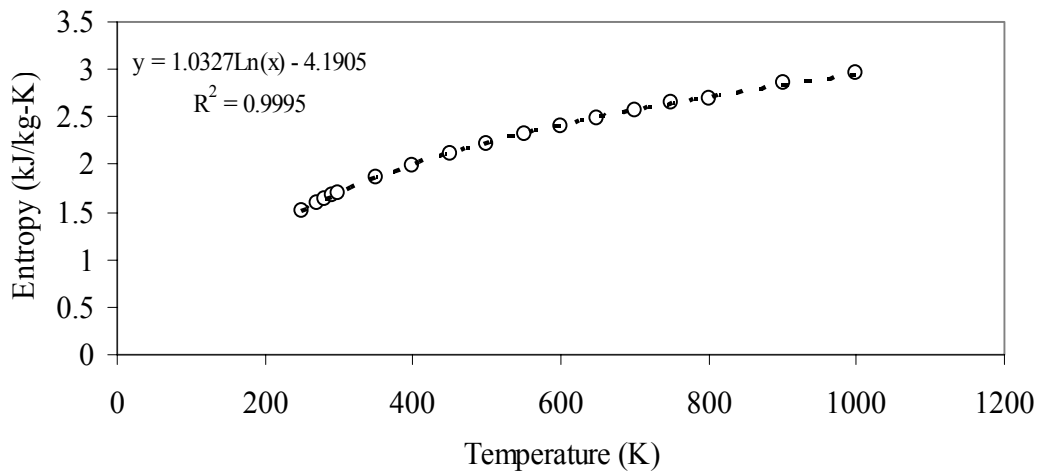


Figure 3. Regression Results for Entropy as a Function of Temperature for Air

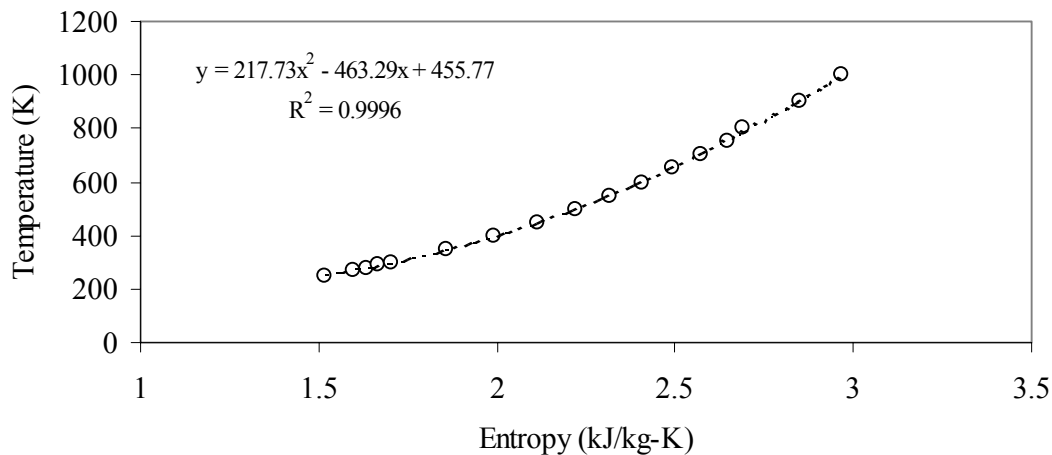


Figure 4. Regression Results for Temperature as a Function of Entropy for Air

For example, if the inlet temperature is 295 K, then the entropy of the inlet air is estimated to be 1.682 kJ/(kg-K). Suppose that the pressure ratio is 6 for a single stage of the compressor and that the molecular weight of air is approximately 29, based on an example case study reported in Wark (1993). The estimated outlet air entropy will be 2.196 kJ/(kg-K). By comparison, the exact value reported in Wark (1993) for the same case is 2.199 kJ/(kg-K). Thus, the regression-based approach utilized here agrees well with the published case study.

Using the estimate of the entropy of the outlet air, a regression expression shown in Figure 4 is used to estimate the temperature of the outlet air.

$$T_{C,i,out} = 217.73s_{C,i,out}^2 - 463.29s_{C,i,out} + 455.77 \quad (13)$$

In this example, the temperature is estimated to be 488 K, compared to a value of 490 K as reported by Wark (1983). With knowledge of the temperature of the outlet air, the enthalpy of the outlet air is estimated based upon the regression expression shown in Figure 5.

$$h_{C,i,out,isentropic} = 0.0001T^2 + 0.9302T + 11.687 \quad (14)$$

The estimated enthalpy is 489.9 kJ/kg, versus a reported value of 492.7 kJ/kg. This procedure is based upon an isentropic compressor.

To take into account the irreversibilities in an actual compressor, the actual enthalpy of the outlet air is estimated based upon the following relationship:

$$h_{C,i,out} = h_{C,i,in} + \frac{h_{C,i,out,isentropic} - h_{C,i,in}}{\eta_{C,i}} \quad (15)$$

For example, if the adiabatic compressor efficiency for stage i is assumed to be 0.82, then the estimated enthalpy at the outlet of stage i is:

$$h_{C,i,out} = 294.8 + (489.9 - 294.8) / 0.82 = 532.7 \text{ kJ/kg}$$

The value reported by Wark (1983) is 536.1 kJ/kg. Based upon the estimated enthalpy for the actual compressor outlet air, the actual outlet temperature is estimated based upon the regression Equation given in Figure 6.

$$T_{C,i,out} = -9 \times 10^{-5} h_{C,i,out} + 1.0563 h_{C,i,out} - 9.0996 \quad (16)$$

The estimated outlet temperature is 528 K, versus a reported value of 532 K. Thus, although there is some error in the estimation procedure, the result is within a few degrees of the reported value. The outlet temperature of stage i is treated as the inlet temperature of the next stage. The above computation is repeated and the outlet temperature for the last stage can be obtained.

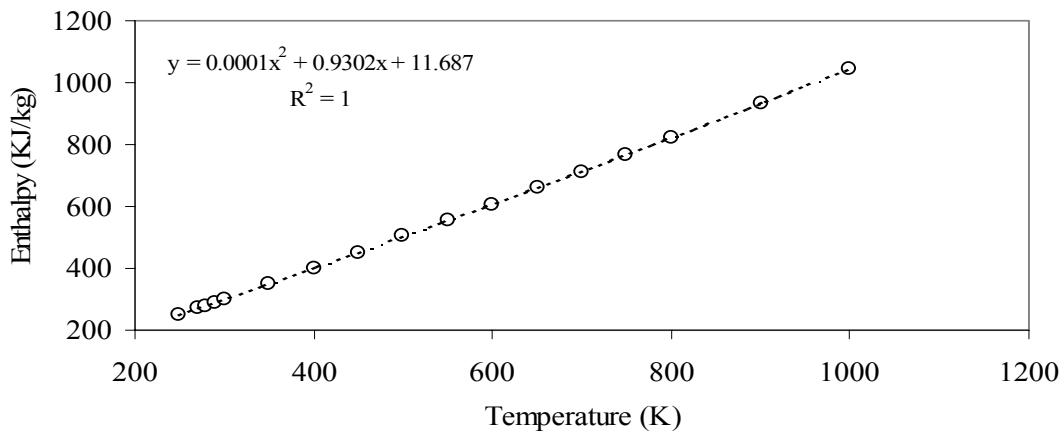


Figure 5. Regression Results for Enthalpy as a Function of Temperature for Air

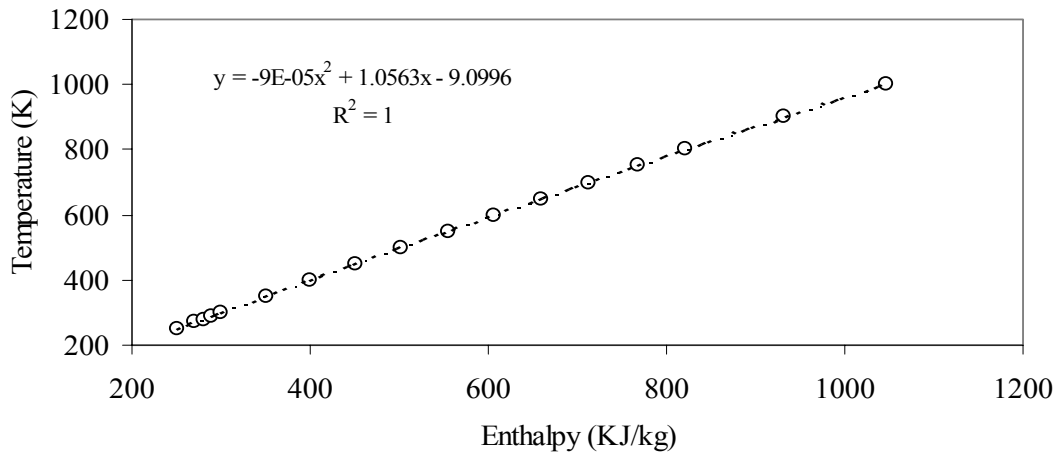


Figure 6. Regression Results for Temperature as a Function of Enthalpy for Air

2.2 Combustor

For the combustor, we assume that in general the fuel contains the following major components:

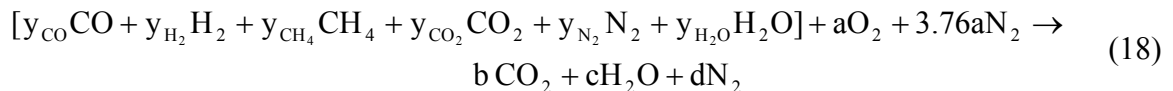
- carbon monoxide (CO)
- hydrogen (H₂)
- methane (CH₄)
- carbon dioxide (CO₂)
- nitrogen (N₂)
- water vapor (H₂O)

Although syngas may also contain relatively small amounts of hydrogen sulfide (H₂S), carbonyl sulfide (COS), and ammonia (NH₃), we will assume that these three components contribute negligibly to the mass and energy balance. These latter three components are significant in terms of the formation of SO₂ and NO_x emissions.

The volume percent (or, equivalently, mole fraction) of each of the six major components will be known. Therefore, a heating value can be estimated for the fuel. Based upon data reported by Flagan and Seinfeld (1988), the enthalpy of reaction of CO is estimated as 283,400 J/gmole, the enthalpy of reaction of H₂ is estimated as 242,200 J/gmole, and the enthalpy of reaction of CH₄ is estimated as 803,500 J/gmole. These are estimated on a lower heating value basis, assuming that H₂O produced is in the form of vapor. The other three major components are assumed to be non-reactive. The heating value of the fuel gas, on a J/gmole basis, is given by:

$$\Delta h_{r,\text{fuel}} = y_{\text{CO}} \Delta h_{r,\text{CO}} + y_{\text{H}_2} \Delta h_{r,\text{H}_2} + y_{\text{CH}_4} \Delta h_{r,\text{CH}_4} \quad (17)$$

The syngas is represented by a mixture of the six constituent gases. Air is a mixture primarily of oxygen and nitrogen. For every mole of oxygen in the air, there are approximately 3.76 moles of nitrogen. The major products of combustion are carbon dioxide, water vapor, nitrogen, and excess oxygen. Therefore, the mass balance for stoichiometric combustion is given by:



The mass balance is given on the basis of one mole of syngas mixture. Thus, the units of each stoichiometric coefficient are moles of the respective compound per mole of syngas mixture. The mole fractions of each component in the syngas are known. Therefore, the unknowns are the stoichiometric coefficients a, b, c, and d. These can be solved using elemental balances:

Carbon:	$y_{\text{CO}} + y_{\text{CH}_4} + y_{\text{CO}_2} = b$
Hydrogen:	$2y_{\text{H}_2} + 4y_{\text{CH}_4} + 2y_{\text{H}_2\text{O}} = 2c$
Oxygen:	$y_{\text{CO}} + 2y_{\text{CO}_2} + y_{\text{H}_2\text{O}} + 2a = 2b + c$
Nitrogen	$2y_{\text{N}_2} + 2(3.76)a = 2d$

Based upon these four Equations, the solutions for a, b, c, and d are:

$$a = \frac{1}{2}y_{H_2} + 2y_{CH_4} + \frac{1}{2}y_{CO} \quad (19)$$

$$b = y_{CO} + y_{CH_4} + y_{CO_2} \quad (20)$$

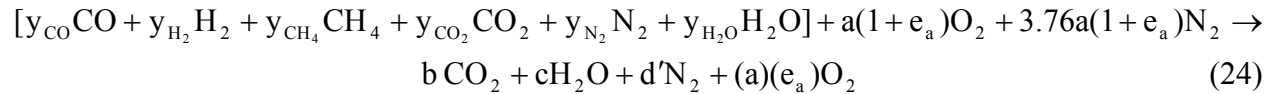
$$c = y_{H_2} + 2y_{CH_4} + y_{H_2O} \quad (21)$$

$$d = y_{N_2} + 3.76a \quad (22)$$

However, gas turbine combustors operate with a significant amount of excess air. The mass balance for the case with excess air can be developed based upon the stoichiometric mass balance by introducing a new variable for the fraction of excess air, e_a . The fraction of excess air is given by:

$$e_a = \frac{(Total\ air - stoichiometric\ air)}{(Stoichiometric\ air)} \quad (23)$$

The mass balance for excess air is:



The solutions for a, b, and c are the same as in Equations (12), (13), and (14). The solution for d is replaced by the solution for d':

$$d' = y_{N_2} + 3.76a(1 + e_a) \quad (25)$$

For example, suppose that a fuel contains, on a mole or volume percentage basis, 24.8% hydrogen, 39.5 % carbon dioxide, 1.5 % methane, 9.3 % carbon dioxide, 2.3 % nitrogen, and 22.7 % water vapor. Stoichiometric combustion of this fuel would require 0.3515 moles of oxygen per mole of syngas mixture, and 1.32 moles of nitrogen in the inlet air. The exhaust gas would contain 0.50 moles of carbon dioxide, 0.50 moles of water vapor, and 1.34 moles of nitrogen, all based upon one mole of syngas combusted. If the fuel were burned with 100

percent excess air, then the exhaust gas would contain 0.50 moles of carbon dioxide, 0.50 moles of water vapor, 2.67 moles of nitrogen, and 0.35 moles of oxygen, all based upon one mole of syngas combusted.

The actual amount of air that is needed to combust the fuel depends upon the desired turbine inlet temperature. Therefore, it is necessary to solve an energy balance in order to estimate the fuel to air ratio. The turbine inlet temperature, $T_{T,in}$, is a known design parameter. The temperature of the air from the compressor is known based upon the compressor pressure ratio and adiabatic compressor efficiency, as explained in the previous section. The syngas temperature would also be known. The only unknown is the excess air ratio. Thus, the energy balance is:

$$\begin{aligned} & bH_{CO_2}(T_{T,in}) + cH_{H_2O}(T_{T,in}) + d'H_{N_2}(T_{T,in}) + (a)(e_a)H_{O_2}(T_{T,in}) - \\ & [y_{CO}H_{CO}(T_{SG}) + y_{H_2}H_{H_2}(T_{SG}) + y_{CH_4}H_{CH_4}(T_{SG}) + \\ & y_{CO_2}H_{CO_2}(T_{SG}) + y_{N_2}H_{N_2}(T_{SG}) + y_{H_2O}H_{H_2O}(T_{SG})] - \\ & a(1 + e_a)H_{O_2}(T_{C,out}) - 3.76a(1 + e_a)H_{N_2}(T_{C,out}) = \Delta h_{r,SG} \end{aligned} \quad (26)$$

Because all of the terms in this equation are known except for the excess air fraction, the equation can be rearranged in terms of excess air fraction as follows:

$$\begin{aligned} & bH_{CO_2}(T_{T,in}) + cH_{H_2O}(T_{T,in}) + \{y_{N_2} + 3.76a(1 + e_a)\}H_{N_2}(T_{T,in}) + (a)(e_a)H_{O_2}(T_{T,in}) - \\ & [y_{CO}H_{CO}(T_{SG}) + y_{H_2}H_{H_2}(T_{SG}) + y_{CH_4}H_{CH_4}(T_{SG}) + \\ & y_{CO_2}H_{CO_2}(T_{SG}) + y_{N_2}H_{N_2}(T_{SG}) + y_{H_2O}H_{H_2O}(T_{SG})] - \\ & a(1 + e_a)H_{O_2}(T_{C,out}) - 3.76a(1 + e_a)H_{N_2}(T_{C,out}) = \Delta h_{r,SG} \end{aligned} \quad (27)$$

For convenience, we create the following groups of terms:

$$\begin{aligned} H_{fuel} = & y_{CO}H_{CO}(T_{SG}) + y_{H_2}H_{H_2}(T_{SG}) + y_{CH_4}H_{CH_4}(T_{SG}) + \\ & y_{CO_2}H_{CO_2}(T_{SG}) + y_{N_2}H_{N_2}(T_{SG}) + y_{H_2O}H_{H_2O}(T_{SG}) \end{aligned} \quad (28)$$

$$H_{air,stoich} = aH_{O_2}(T_{C,out}) + 3.76aH_{N_2}(T_{C,out}) \quad (29)$$

$$H_{products,stoich} = bH_{CO_2}(T_{T,in}) + cH_{H_2O}(T_{T,in}) + \{y_{N_2} + 3.76a\}H_{N_2}(T_{T,in}) \quad (30)$$

The solution for the excess air fraction is given by:

$$e_a = \frac{H_{\text{fuel}} + H_{\text{air,stoich}} + \Delta h_{r,\text{fuel}} - H_{\text{products,stoich}}}{a [3.76 \{H_{\text{N}_2}(T_{\text{T,in}}) - H_{\text{N}_2}(T_{\text{C,out}})\} + \{H_{\text{O}_2}(T_{\text{T,in}}) - H_{\text{O}_2}(T_{\text{C,out}})\}]} \quad (31)$$

For example, suppose that the turbine inlet temperature is specified as 1,100 K. For the same syngas composition as previously assumed, and for the same compressor outlet temperature of 528 K, the estimated excess air ratio is 4.218. This excess air ratio was verified in two ways. First, the excess air ratio was substituted into the final mass balance, and an energy balance was calculated using Equation (19). The energy balance was properly closed. Second, the same assumptions were input into an independently developed spreadsheet that uses a different set of equations for estimating enthalpy. The results agreed to within a few degrees for the predicted turbine inlet temperature calculated by the independent software.

After the computation of excess air, the molar fraction per mole fuel gas of exhaust gas for the combustor can be estimated.

$$y_{\text{ex,CO}_2} = y_{\text{CO}} + y_{\text{CH}_4} + y_{\text{CO}_2} \quad (32)$$

$$y_{\text{ex,H}_2\text{O}} = y_{\text{H}_2} + 2y_{\text{CH}_4} + y_{\text{H}_2\text{O}} \quad (33)$$

$$y_{\text{ex,N}_2} = y_{\text{N}_2} + 3.76(1 + e_a) \left(\frac{1}{2} y_{\text{H}_2} + 2y_{\text{CH}_4} + \frac{1}{2} y_{\text{CO}} \right) \quad (34)$$

$$y_{\text{ex,O}_2} = e_a \left(\frac{1}{2} y_{\text{H}_2} + 2y_{\text{CH}_4} + \frac{1}{2} y_{\text{CO}} \right) \quad (35)$$

From Equation (1) in Section 2.0, the mass flow of exhaust gas out of the combustor or at the turbine inlet can be estimated. The actual and reference pressures in the turbine inlet are $P_{\text{ref}} = P_{\text{act}} = P_{\text{T,in}}$. For a specific design basis, the actual and reference temperatures are $T_{\text{act}} = T_{\text{ref}} = 2,880$ °R, which are converted from the firing temperature of 2,420 °F for a Frame 7FA+e gas turbine (Gebhardt, 2000). According to Equations (25) to (28), the molecular weight of mixture gas at the inlet of the turbine can be estimated as:

$$MW_{act} = y_{ex,CO_2} MW_{CO_2} + y_{ex,H_2O} MW_{H_2O} + y_{ex,N_2} MW_{N_2} + y_{ex,O_2} MW_{O_2} \quad (36)$$

The reference molecular weight is assumed to be $MW_{ref} = 28.4$. Therefore, the actual mass flow in the turbine inlet can be calculated by Equation (1). The reference mass flow is calibrated to make the result of the power output match the published value. The total mass flow through the combustor is the sum of the combustor air mass flow and fuel gas mass flow, which is the same as the actual mass flow to the turbine.

$$m_{fuel} + m_{comb,air} = m_{act} \quad (37)$$

The mass flow of fuel gas is calculated using the following equations. First, the molecular weight of fuel gas can be estimated as:

$$MW_{fuel} = y_{CO} MW_{CO} + y_{H_2} MW_{H_2} + y_{CH_4} MW_{CH_4} + y_{CO_2} MW_{CO_2} + y_{N_2} MW_{N_2} + y_{H_2O} MW_{H_2O} \quad (38)$$

The ratio of fuel to air required for combustion can be calculated as:

$$r_{f,air} = \frac{MW_{fuel}}{a(1 + e_a) MW_{O_2} + 3.76 a(1 + e_a) MW_{N_2}} \quad (39)$$

Since the actual mass flow to the turbine is the sum of combustor air mass flow and fuel gas mass flow, the mass ratio of fuel and the actual mass flow to the turbine is:

$$r_{f,act} = \frac{r_{f,air}}{1 + r_{f,air}} \quad (40)$$

Therefore, the mass flow of fuel can be estimated as:

$$m_{fuel} = m_{act} \times r_{f,act} \quad (41)$$

The mole flow rate of fuel gas is estimated based on the following equation:

$$M_{fuel} = \frac{m_{fuel}}{MW_{fuel}} \quad (42)$$

The combustor air mass flow is estimated as:

$$m_{comb,air} = m_{act} - m_{fuel} \quad (43)$$

Therefore, based on Equation (12) and the combustor air mass flow, the total mass flow of air to the combustor is estimated as:

$$m_{\text{air}} = \frac{m_{\text{act}} - m_{\text{fuel}}}{1 - f_{a,1} - f_{a,2} - f_{a,3}} \quad (44)$$

2.3 Turbine

The energy balance for the turbine is estimated in a manner similar to that for the compressor. However, a key difference is that the exhaust gas is not air, and therefore the thermodynamic data for air is not applicable for use with the turbine. In addition, pressure losses in the combustor and the turbine back pressure must be accounted for when estimating the work capability of the turbine.

The turbine consists of three stages. The cooling air from the compressor is injected into the outlet flow from each stage. The conceptual diagram is shown in Figure 7. The pressure at the combustor outlet, which is assumed to be the same as the turbine inlet pressure, is given by:

$$P_{C,\text{out}} = P_{T,\text{in}} = P_a(r_p) - \Delta p_{\text{comb}} \quad (45)$$

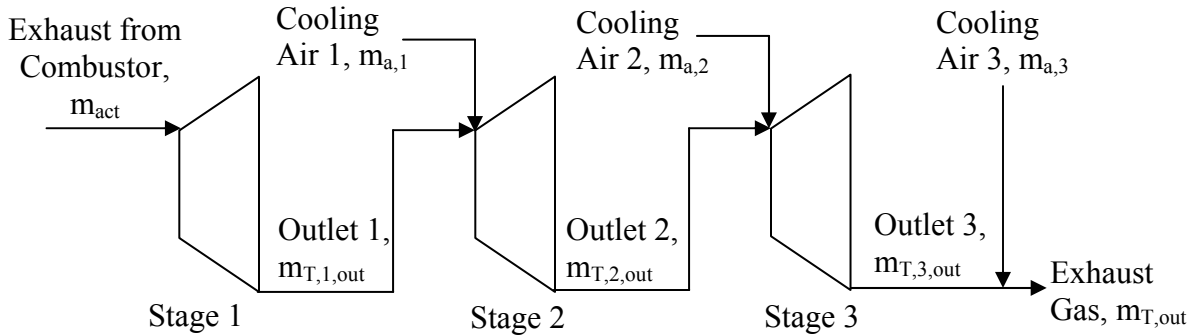


Figure 7. Simplified Diagram of a Three-Stage Turbine

The pressure at the turbine outlet is given by:

$$P_{T,\text{out}} = P_a + \Delta p_{\text{back}} \quad (46)$$

Therefore, the pressure ratio for the turbine is given by:

$$r_{p,turb} = \frac{P_{T,in}}{P_{T,out}} = \frac{(P_a r_p - \Delta p_{comb})}{(P_a + \Delta p_{back})} \quad (47)$$

The pressure ratio for each stage of the turbine is the same and is estimated as:

$$r_{p,turb,i} = (r_{p,turb})^{0.33} \quad (48)$$

For each stage, the outlet pressure is estimated as:

$$P_{T,1,out} = \frac{P_{T,in}}{(r_{p,turb})^{0.33}} \quad (49)$$

$$P_{T,2,out} = \frac{P_{T,in}}{(r_{p,turb})^{0.67}} \quad (50)$$

$$P_{T,3,out} = \frac{P_{T,in}}{r_{p,turb}} \quad (51)$$

For each stage of the turbine, the cooling air is injected and mixed with the exhaust from the previous stage. Therefore, the mass flow rate through each stage and at the turbine outlet is:

$$m_{T,1,out} = m_{act} \quad (52)$$

$$m_{T,2,out} = m_{act} + m_{air} f_{a,1} \quad (53)$$

$$m_{T,3,out} = m_{act} + m_{air} (f_{a,1} + f_{a,2}) \quad (54)$$

$$m_{T,out} = m_{act} + m_{air} (f_{a,1} + f_{a,2} + f_{a,3}) \quad (55)$$

For each stage, the turbine outlet temperature is calculated. Because nitrogen comprises approximately 70 percent or more (by volume) of the exhaust gases from the gas turbine, we use nitrogen as the basis for the calculations to determine the turbine exhaust temperature. Figures 8 and 9 display the regression equations for entropy as a function of temperature, and for temperature as a function of entropy, respectively. The entropy at the turbine inlet is estimated based upon the turbine inlet temperature.

$$s_{T,i,in} = 3.0044T^{0.1443} \quad (56)$$

For example, if the turbine inlet temperature is 1,100 K, then the estimated entropy from the equation in Figure 8 is 8.253 kJ/kg-K. The entropy at the stage outlet is estimated as:

$$s_{T,i,out} = s_{T,i,in} + \left(\frac{R}{MW_{N_2}}\right)\ln\left(\frac{1}{r_{P,i,turb}}\right) \quad (57)$$

If the stage pressure ratio is equal to 6, then the entropy is estimated to be:

$$s_{T,i,out} = 8.253 + 8.3144/28 \ln(1/6) = 7.721 \text{ kJ/kg-K}$$

At this value of entropy, the turbine outlet temperature is calculated, based upon the regression equation given in Figure 9.

$$T_{T,i,out} = 4.9161 \times 10^{-4} (s_{T,i,out})^{6.9277} \quad (58)$$

The temperature is estimated to be 694 K. This temperature is exactly the same as that reported by Wark (1983) for a similar calculation based upon air. If the turbine is not isentropic, then the turbine outlet temperature will be higher than the predicted value based upon isentropic calculation.

The isentropic turbine work output is given by the difference between the enthalpies of the inlet and outlet under isentropic conditions. The enthalpy of exhaust gas is estimated based on the regression equation shown in Figure 10.

$$h_{T,i, out, isentropic} = 5.9731 \times 10^{-5} T^2 + 1.0373 T - 10.1939 \quad (59)$$

The estimated enthalpy is 738.5kJ/kg when the outlet temperature is 694 K. This procedure is based on an isentropic turbine. If the inlet temperature is 1,100 K, then the enthalpy at turbine inlet is estimated to be:

$$h_{T, in} = 5.9731 \times 10^{-5} \times 1100^2 + 1.0373 \times 1100 - 10.1939 = 1,203.1 \text{ kJ/kg}$$

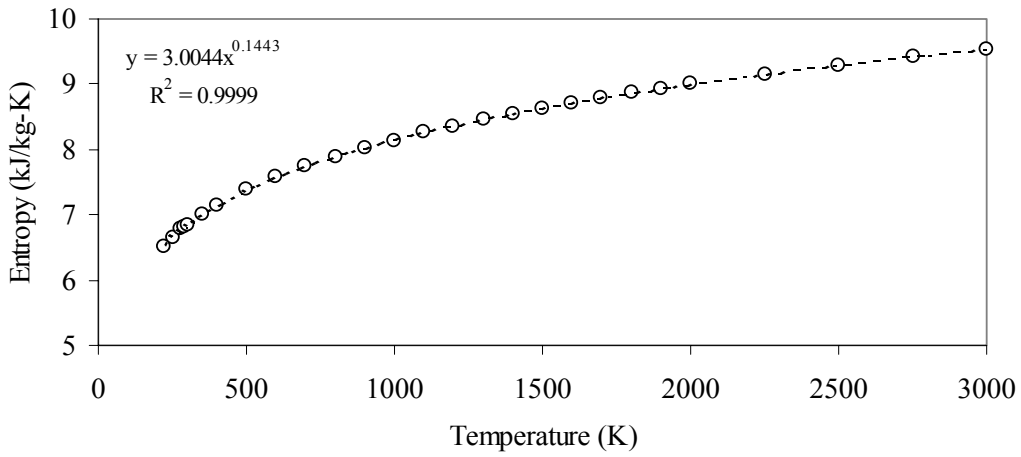


Figure 8. Regression Results for Entropy as a Function of Temperature for Nitrogen (N₂)

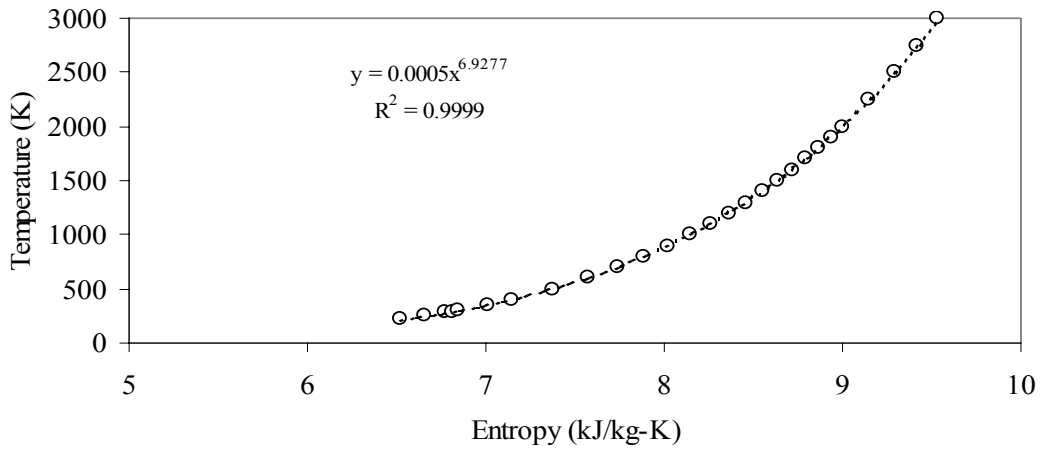


Figure 9. Regression Results for Temperature as a Function of Entropy for Nitrogen (N₂)

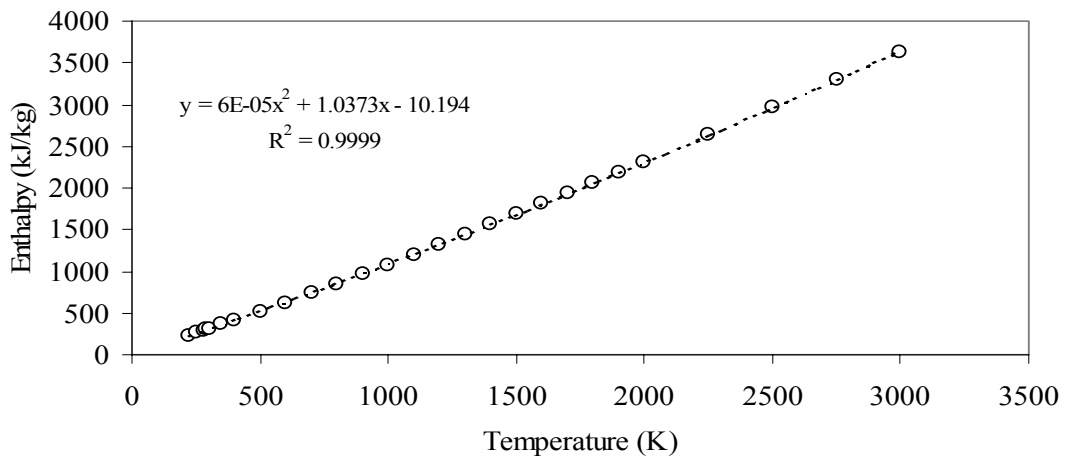


Figure 10. Regression Results for Enthalpy as a Function of Temperature for Nitrogen (N₂)

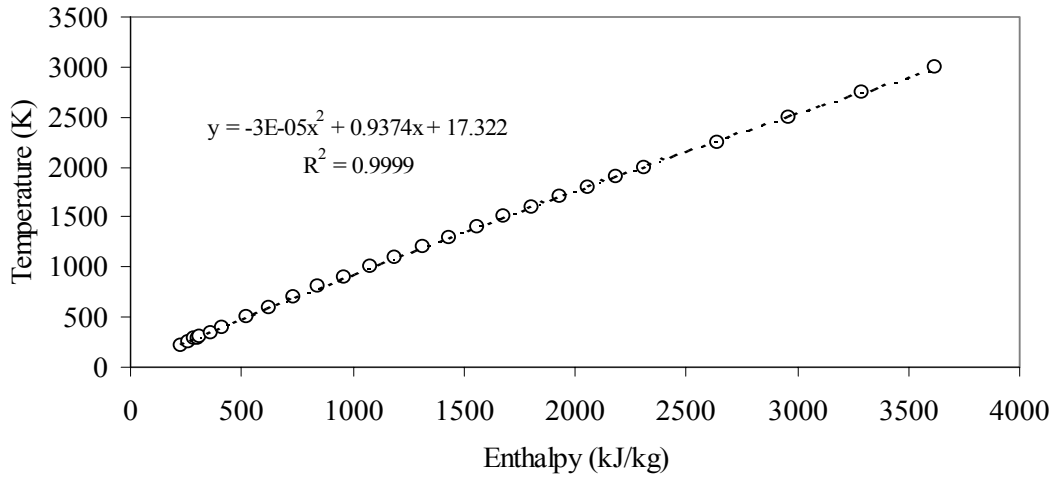


Figure 11. Regression Results for Temperature as a Function of Enthalpy for Nitrogen (N₂)

To take into account the efficiency of an actual expander, the actual enthalpy of the outlet gas is estimated based on the following relationship:

$$h_{T,i,out} = h_{T,i,in} + (h_{T,i,out, isentropic} - h_{T,i,in})\eta_{Ti} \quad (60)$$

If the adiabatic turbine efficiency is assumed to be 0.95, then the estimated enthalpy at the turbine outlet is:

$$h_{T,i,out} = 1,203.1 + (738.5 - 1,203.1) \times 0.95 = 761.7 \text{ kJ/kg}$$

The actual temperature at the stage outlet is estimated based upon the regression expression shown in Figure 11.

$$T_{T,i,out} = -3.2769 \times 10^{-5} h_{T,i,out}^2 + 0.9347 h_{T,i,out} + 17.3221 \quad (61)$$

After each stage, the cooling air is mixed with the exhaust flow. The mixture temperature is estimated based on the specific heat and the mass flow of the streams in the mixture:

$$T_{T,i+1,in} = \frac{(m_{air} f_{a,i}) c_{p,air} T_{a,i} + m_{T,i,out} c_{p,i,out} T_{T,i,out}}{(m_{air} f_{a,i}) c_{p,air} + m_{T,i,out} c_{p,i,out}} \quad (62)$$

The mixture temperature is treated as the inlet temperature for next the stage. After the third stage of the turbine, the mixture temperature is the exhaust temperature of the gas turbine.

2.4 Net Power Output

The net electricity power produced by the gas turbine is based on the net shaft energy produced by the turbine minus the shaft energy consumed by the compressor.

The compressor work requirement is estimated based on the amount of air needed per mole fuel gas combusted and the enthalpy difference between the outlet and inlet of the compressor. The air mainly consists of nitrogen and oxygen and other minor components are ignored. Using the IECM enthalpy function, the oxygen and nitrogen enthalpies are estimated as a function of temperature. For each stage of the compressor, the inlet temperature and the outlet temperature are computed. The enthalpy difference per mole syngas of the first stage is computed as:

$$\Delta h_{C,i} = y_{c,i,air,N_2} [h_{N_2}(T_{C,i,out}) - h_{N_2}(T_{C,i,in})] + y_{c,i,air,O_2} [h_{O_2}(T_{C,i,out}) - h_{O_2}(T_{C,i,in})] \quad (63)$$

For the first stage, the flow fraction of nitrogen and oxygen per mole syngas is estimated as:

$$y_{c,1,air,O_2} = \frac{a(1 + e_a)}{1 - f_{a,1} - f_{a,2} - f_{a,3}} \quad (64)$$

$$y_{c,1,air,N_2} = 3.76 y_{c,1,air,O_2} \quad (65)$$

Since the nitrogen flow rate can be computed based on that of oxygen, only the computation of the oxygen flow fraction is listed for the other stages. For the second and the third stages, the oxygen molar fraction per mole syngas is estimated as:

$$y_{c,2,air,O_2} = \frac{a(1 + e_a)(1 - f_{a,1})}{1 - f_{a,1} - f_{a,2} - f_{a,3}} \quad (66)$$

$$y_{c,3,air,O_2} = \frac{a(1 + e_a)(1 - f_{a,1} - f_{a,2})}{1 - f_{a,1} - f_{a,2} - f_{a,3}} \quad (67)$$

Therefore, the total enthalpy difference for the compressor is:

$$\Delta h_c = \Delta h_{c,1} + \Delta h_{c,2} + \Delta h_{c,3} \quad (68)$$

From each stage, part of the air is extracted from the outlet air and injected into the turbine for cooling. The cooling air molar flow per mole syngas is computed as:

$$y_{a,i,O_2} = \frac{a(1 + e_a) f_{a,i}}{1 - f_{a,1} - f_{a,2} - f_{a,3}} \quad (69)$$

The turbine work is estimated based on the amount of exhaust gas produced per mole fuel. The exhaust gas mainly consists of carbon dioxide (CO₂), steam (H₂O), nitrogen (N₂), and oxygen (O₂). The enthalpy functions of carbon dioxide and steam are listed in Appendix I. The amount of exhaust gas per mole fuel is estimated based on the equations in the combustor section. The inlet temperature and the outlet temperature for each stage of the turbine are estimated in the previous section. The enthalpy difference per mole syngas in each stage is estimated as:

$$\begin{aligned} \Delta h_{T,i} = & y_{T,i,CO_2} [h_{CO_2}(T_{T,i,in}) - h_{CO_2}(T_{T,i,out})] + y_{T,i,H_2O} [h_{H_2O}(T_{T,i,in}) - h_{H_2O}(T_{T,i,out})] \\ & + y_{T,i,N_2} [h_{N_2}(T_{T,i,in}) - h_{N_2}(T_{T,i,out})] + y_{T,i,O_2} [h_{O_2}(T_{T,i,in}) - h_{O_2}(T_{T,i,out})] \end{aligned} \quad (70)$$

For the first stage, the mass flow of each component per mole syngas is the same as that of the exhaust gas from the combustor, which is computed in Equations (32) to (35). For carbon dioxide and steam, the flow rates per mole syngas are the same in each of the three stages.

$$y_{T,i,CO_2} = y_{CO} + y_{CH_4} + y_{CO_2} \quad (71)$$

$$y_{T,i,H_2O} = y_{H_2} + 2y_{CH_4} + y_{H_2O} \quad (72)$$

The flow rates of nitrogen and oxygen are changed by air injection from the compressor. Therefore, the amount of each gas per mole syngas for each stage is:

$$y_{T,i,N_2} = y_{N_2} + 3.76(1 + e_a) \left(\frac{1}{2} y_{H_2} + 2y_{CH_4} + \frac{1}{2} y_{CO} \right) \quad (73)$$

$$y_{T,2,N_2} = y_{N_2} + 3.76(1 + e_a)\left(\frac{1}{2}y_{H_2} + 2y_{CH_4} + \frac{1}{2}y_{CO}\right) + 3.76y_{a,1,O_2} \quad (74)$$

$$y_{T,3,N_2} = y_{N_2} + 3.76(1 + e_a)\left(\frac{1}{2}y_{H_2} + 2y_{CH_4} + \frac{1}{2}y_{CO}\right) + 3.76(y_{a,1,O_2} + y_{a,2,O_2}) \quad (75)$$

$$y_{T,1,O_2} = e_a\left(\frac{1}{2}y_{H_2} + 2y_{CH_4} + \frac{1}{2}y_{CO}\right) \quad (76)$$

$$y_{T,2,O_2} = e_a\left(\frac{1}{2}y_{H_2} + 2y_{CH_4} + \frac{1}{2}y_{CO}\right) + y_{a,1,O_2} \quad (77)$$

$$y_{T,3,O_2} = e_a\left(\frac{1}{2}y_{H_2} + 2y_{CH_4} + \frac{1}{2}y_{CO}\right) + (y_{a,1,O_2} + y_{a,2,O_2}) \quad (78)$$

For the exhaust from the turbine, the nitrogen and oxygen flows are given by:

$$y_{T,out,N_2} = y_{N_2} + 3.76(1 + e_a)\left(\frac{1}{2}y_{H_2} + 2y_{CH_4} + \frac{1}{2}y_{CO}\right) + 3.76(y_{a,1,O_2} + y_{a,2,O_2} + y_{a,3,O_2}) \quad (79)$$

$$y_{T,out,O_2} = e_a\left(\frac{1}{2}y_{H_2} + 2y_{CH_4} + \frac{1}{2}y_{CO}\right) + (y_{a,1,O_2} + y_{a,2,O_2} + y_{a,3,O_2}) \quad (80)$$

Therefore, the total enthalpy difference for the compressor is:

$$\Delta h_T = \Delta h_{T,1} + \Delta h_{T,2} + \Delta h_{T,3} \quad (81)$$

The net shaft work per mole fuel is estimated based on the differences in work between the compressor and turbine. Furthermore, the generator is subject to inefficiencies. The generator efficiency η_s can be calibrated to calculate the actual generator output. Therefore, the actual shaft work is estimated as:

$$Q_S = (\Delta h_T - \Delta h_C)\eta_S M_{fuel} \quad (82)$$

where the shaft work is in units of BTU/hr.

The lower heating value (LHV) of fuel is estimated to be:

$$\text{LHV} = \frac{\Delta h_{r,SG}}{\text{MW}_{\text{fuel}}} \quad (83)$$

The total energy input of the system is estimated based on the heating value and the mass flow of fuel:

$$Q_{\text{fuel}} = m_{\text{fuel}} \text{LHV} \quad (84)$$

The simple cycle efficiency is computed as:

$$\eta_{SC} = \frac{Q_S}{Q_{\text{fuel}}} \quad (85)$$

The net electricity produced in the simple cycle is estimated to be:

$$W_{SC} = 3.414 H_S M_{\text{fuel}} \quad (86)$$

where the net electricity is in units of MW.

3.0 Combined Cycle Gas Turbine Mass and Energy Balance

A combined cycle gas turbine (CCGT) is comprised of a gas turbine and a steam cycle. The gas turbine model has been introduced in the previous section. The steam cycle consists of a heat recovery steam generator, a steam turbine, and other auxiliary parts. The exhaust gas from the gas turbine flows through a series of heat exchangers in the HRSG. The high temperature exhaust gas from the gas turbine is cooled to heat superheated steam, saturated steam, and boiler feedwater via a series of heat exchangers. The cooled flue gas is exhausted from the stack. A substantial portion of the steam is sent to the steam turbine and expanded through several stages. The shaft work is converted into electricity by the generator. The combined cycle system overall performance model is presented in this section.

The energy recovered from the exhaust gas into the HRSG is estimated by the difference in inlet and outlet exhaust gas enthalpy. The exhaust gas mainly consists of carbon dioxide (CO₂), steam (H₂O), nitrogen (N₂), and oxygen (O₂). The HRSG inlet temperature is the gas turbine outlet temperature. Thus, the HRSG outlet temperature is known. The equations for enthalpy computation have been introduced in the previous section. The total enthalpy difference associated with heat recovery per mole fuel gas is estimated based on the exhaust from the turbine:

$$\begin{aligned}\Delta h_H &= y_{T,out,CO_2} \Delta h_{CO_2} + y_{T,out,H_2O} \Delta h_{H_2O} + y_{T,out,N_2} \Delta h_{N_2} + y_{T,out,O_2} \Delta h_{O_2} \\ &= y_{T,out,CO_2} [h_{CO_2}(T_{T,out}) - h_{CO_2}(T_{H,out})] + y_{T,out,H_2O} [h_{H_2O}(T_{T,out}) - h_{H_2O}(T_{H,out})] \\ &\quad + y_{T,out,N_2} [h_{N_2}(T_{T,out}) - h_{N_2}(T_{H,out})] + y_{T,out,O_2} [h_{O_2}(T_{T,out}) - h_{O_2}(T_{H,out})]\end{aligned}\quad (87)$$

For a natural gas fueled combined cycle, the total energy input to the HRSG or the steam cycle is:

$$Q_{H,NGCC} = \Delta h_H M_{fuel} \quad (88)$$

where the energy input is in units of BTU/hr.

For a combined cycle used in an IGCC plant, the total heat input to the HRSG should take into account the heat obtained from high and low temperature cooling of syngas between the gasifier outlet and the gas turbine inlet. In addition, the thermal energy due to steam or water

injection, for purposes of syngas humidification, should be deducted. A significant fraction of the thermal energy from the gas cooling is recovered to generate steam and hot water for the steam cycle. Buchanan *et al.* (1998) mentioned that the high pressure saturated steam is generated in the gas cooler and is joined with the main steam supply. A similar process for syngas cooling is also described by Bechtel *et al.* (2002). Since there is some heat loss in the process of syngas cooling and part of the heat is used in other process, it is assumed that 90% of the heat from syngas cooling is recovered in the steam cycle. This assumption is discussed in Section 4.2.

$$Q_{H,IGCC} = \Delta h_H M_{\text{fuel}} + f_{\text{cooling}} \Delta h_{\text{cooling}} M_{\text{fuel}} - h_{\text{moisture}} \quad (89)$$

The heat from gas cooling is computed based on the clean dry syngas composition and the temperature drop during cooling. Assuming that the syngas at the exit temperature of a gasifier is cooled down to the inlet temperature of the combustor, and that the cleaned syngas composition is known, the sensible heat is estimated as:

$$\begin{aligned} \Delta h_{\text{cooling}} &= y_{\text{CH}_4} \Delta h_{\text{CH}_4} + y_{\text{CO}_2} \Delta h_{\text{CO}_2} + y_{\text{CO}} \Delta h_{\text{CO}} + y_{\text{H}_2} \Delta h_{\text{H}_2} + y_{\text{N}_2} \Delta h_{\text{N}_2} \\ &= y_{\text{CH}_4} [h_{\text{CH}_4}(T_{\text{G,out}}) - h_{\text{CH}_4}(T_{\text{fuel,in}})] + y_{\text{CO}_2} [h_{\text{CO}_2}(T_{\text{G,out}}) - h_{\text{CO}_2}(T_{\text{fuel,in}})] \\ &\quad + y_{\text{CO}} [h_{\text{CO}}(T_{\text{G,out}}) - h_{\text{CO}}(T_{\text{fuel,in}})] + y_{\text{H}_2} [h_{\text{H}_2}(T_{\text{G,out}}) - h_{\text{H}_2}(T_{\text{fuel,in}})] \\ &\quad + y_{\text{N}_2} [h_{\text{N}_2}(T_{\text{G,out}}) - h_{\text{N}_2}(T_{\text{fuel,in}})] \end{aligned} \quad (90)$$

where,

$T_{\text{G,out}}$ = Syngas temperature at the gasifier outlet (°R)

$T_{\text{fuel,in}}$ = Syngas temperature at the combustor inlet (°R)

The sensible heat of injected steam or water is estimated based on the enthalpy of saturated water and the enthalpy of vaporization. When the water injection is selected, the heat of the water is deducted from the total heat input to the steam cycle. The water in the syngas is heated to steam. The heat for vaporization is from the gas cooling. Therefore, the total heat deduction due to the water injection is the heat of water and the heat of vaporization. When the steam injection is selected, the heat of saturated steam is the same as the sum of the heat of saturated water and vaporization. Therefore, the heat deduction of water injection or steam injection is estimated as the following:

$$\begin{aligned}
h_{\text{moisture}} &= m_{\text{moisture}} h_f(T_{\text{moisture}}) + m_{\text{moisture}} h_{fg}(T_{\text{moisture}}) \\
&= M_{\text{fuel}} \times y_{\text{H}_2\text{O}} \times MW_{\text{H}_2\text{O}} \times h_g(T_{\text{moisture}})
\end{aligned}
\tag{91}$$

where,

$MW_{\text{H}_2\text{O}}$ = Molar Weight of H_2O , 18.015 lb/mole.

h_f = Enthalpy of saturated water (Btu/lb)

h_{fg} = Enthalpy of vaporization (Btu/lb)

h_g = Enthalpy of saturated steam (Btu/lb)

The power generated from the steam turbine in the combined cycle is dependent on the heat rate of the steam cycle, HR:

$$W_{\text{ST}} = \frac{1000 Q_{\text{H}}}{\text{HR}} \tag{92}$$

where the power is in units of MW.

Therefore, the total energy output from the combined cycle is the sum of the electricity generated from the simple cycle gas turbine and that of the steam turbine in the combined cycle.

$$W_{\text{CC}} = W_{\text{SC}} + W_{\text{ST}} \tag{93}$$

The total system energy input is computed based on the simple cycle output and simple cycle efficiency, which is computed in Section 2.4. Therefore, the combined cycle efficiency is computed as:

$$\eta_{\text{CC}} = \frac{W_{\text{CC}} \eta_{\text{SC}}}{W_{\text{SC}}} \tag{94}$$

4.0 Calibration of the Performance Model

This section documents the calibration of the gas turbine model based upon data for “Frame 7F” heavy duty gas turbines fueled with natural gas and syngas. In addition, the results of the sensitivity analysis with alternative syngas compositions are reported.

4.1 Natural Gas

A case study of a combined cycle GE 7FA+e gas turbine was used as the basis for calibrating the gas turbine model. In Table 1, the main specifications for the gas turbine and steam cycle are listed. Natural gas was used as the fuel for this case study. For simplicity, natural gas was assumed to be 100% CH₄. The air extraction from the compressor was assumed to be 12%. The compressor is divided into three stages. The air extraction fractions from three stages are 3%, 3%, and 6%, respectively (Frey and Rubin, 1991). The ambient condition is 288 K (59 F) and 14.7 psia, which are the International Standard Organization (ISO) conditions for the gas turbine industry (Brooks, 2000).

In Table 1, the reference mass flow at the inlet of the turbine, adiabatic compressor efficiency, adiabatic turbine efficiency, and the heat rate of the steam cycle were selected during calibration of the model. In order to calibrate the model, selected parameters were varied to closely match published values for key outputs of system performance. Specifically, the adiabatic efficiency for the turbine and compressor were varied in order to match the published gas turbine exhaust temperature and simple cycle efficiency. The reference mass flow at the turbine inlet was varied in order to match the published power output of the gas turbine. The exhaust temperature affects the heat recovery in the HRSG.

After the reference mass flow and turbine adiabatic efficiency were calibrated, the adiabatic compressor efficiency was varied to match the reported simple cycle efficiency. The simple cycle efficiency affects the fuel use per unit of useful output. The heat rate of the combined cycle was varied to match the published value for combined cycle efficiency because the heat rate of the steam cycle affects the power output of the steam turbine. Thus, four unknown parameters, turbine inlet reference mass flow, adiabatic compressor efficiency, adiabatic turbine efficiency, and the steam cycle heat rate, were varied to match the exact

reported values of four outputs, including simple cycle power output, simple cycle efficiency, exhaust temperature, and combined cycle efficiency. Therefore, there may not

Table 1. Main Input Specifications of the Combined Cycle model

Description	Value
Ambient Pressure, psia	14.7
Ambient Temperature, K	288
Compressor Pressure Ratio	15.7 ^a
Combustor Pressure Drop, psia	4
Turbine Back Pressure, psia	2
Turbine Inlet Temperature, K	1600 ^a
Turbine Inlet Reference Mass Flow, lb/hr	3,159,000 ^b
Cooling Air Extraction Fraction, %	12
Adiabatic Compressor Efficiency	0.9285 ^b
Adiabatic Turbine Efficiency	0.8485 ^b
Shaft/Generator Efficiency	0.98
Steam Cycle Heat Rate, BTU/kWh	8960 ^b
HRSG Outlet Temperature, °F	238 ^c
Fuel Composition, vol%	Value
CH ₄	100

^a Brooks, F.J. (2000), GER-3567H, GE Power Systems

^b Values selected based on a calibration process

^c Bechtel *et al.* (2002). The flue gas temperature is 238 °F in a 7FA+e gas turbine combined cycle.

exist an exact match for other outputs, such as the exhaust mass flow and the combined cycle power output.

The curves shown in Figure 12 represent the calibration process for selecting the adiabatic compressor efficiency and turbine efficiency of a simple cycle gas turbine model. For a GE 7FA gas turbine, the published values include an exhaust temperature of 1,119 F, a simple cycle LHV efficiency of 36.47%, and a power output of 171.7 MW (Brooks, 2000). From Figure 10(a), the adiabatic turbine efficiency of 0.8485 was selected to obtain the desired exhaust temperature. To obtain the simple cycle efficiency of 36.47%, the adiabatic compressor efficiency of 0.9285 was selected. After selecting the adiabatic efficiencies for the turbine and compressor, the reference mass flow at the turbine inlet was adjusted to obtain the desired power output. The estimated power output for a simple cycle system was 171.7 MW.

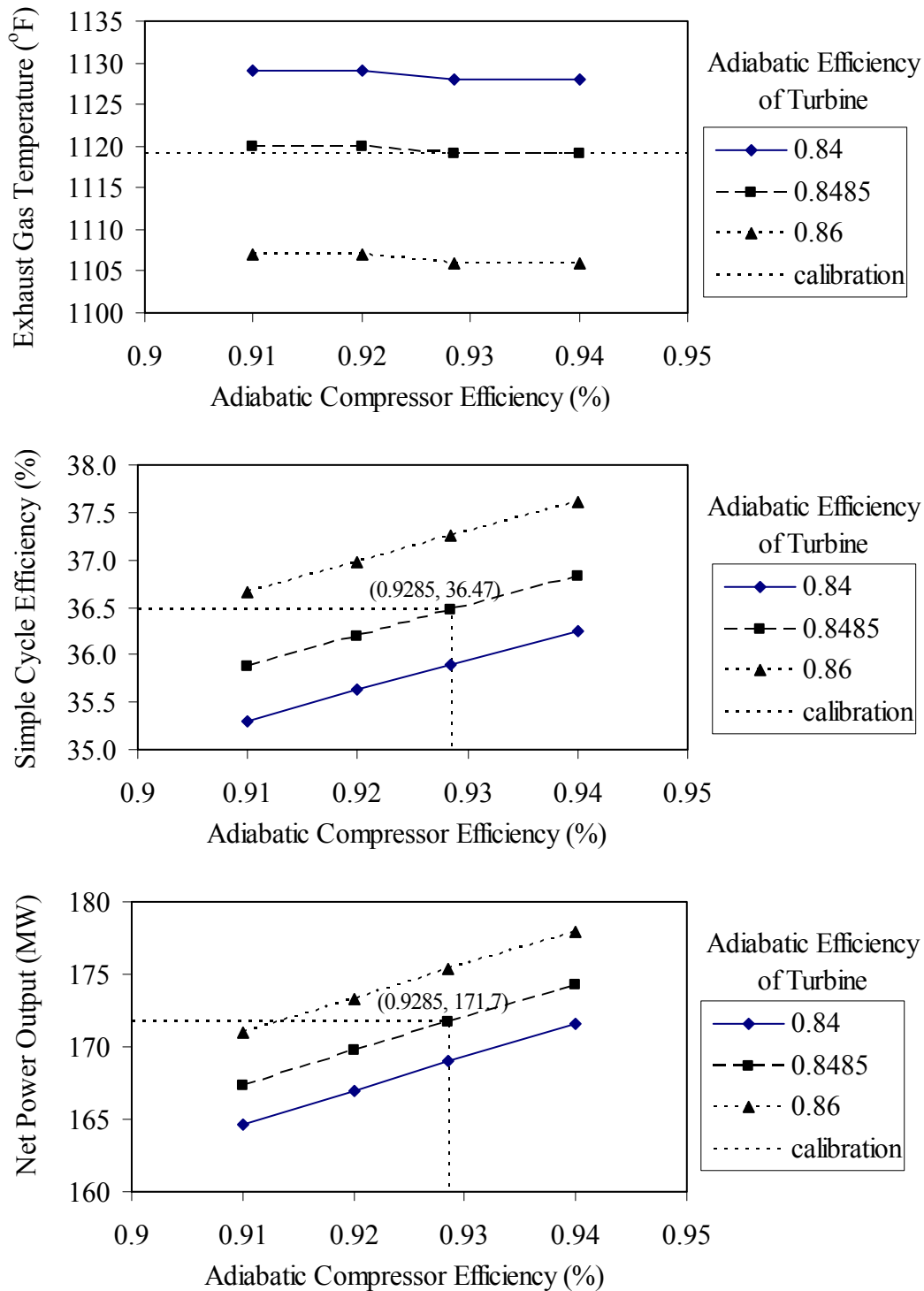


Figure 12. Calibration of the Gas Turbine Model – plots of (a) Exhaust Temperature, (b) Simple Cycle Efficiency, and (c) Simple Cycle Output versus Adiabatic Compressor Efficiency of Gas Turbine.

Note: ET = Adiabatic Turbine Efficiency of Gas Turbine

Table 2. Main Results and Comparison to Published Value based on Natural Gas

Variable	Predicted	Published Value ^a	Relative Difference
Simple Cycle Heat Rate, BTU/kWh	9,360	9,360	0
Gas Turbine Power Output, MW	171.7	171.7	0
Air Flow, lb/hr	3,499,800	3,431,000 ^b	2.0%
Exhaust Flow, lb/hr	3,574,000	3,543,000	0.9%
Exhaust Temperature, °F	1,119	1,119	0
Combined Cycle Power Output, MW	266.0	262.6	1.3%
Combined Cycle Efficiency, %LHV	56.5	56.5	0

^a Brooks, F.J. (2000), GER-3567H, GE Power Systems.

^b Matta, *et al.* (2000), GER-3935B, GE Power Systems

Results based on natural gas match the published data reasonably well, as shown in Table 2. The predicted values for the simple cycle heat rate, simple cycle power output, exhaust temperature, and combined cycle efficiency are exactly the same as the published values because of the calibration process. The relative differences between predicted and reported gas turbine exhaust flow and combined cycle power output are only approximately one to two percent. The results indicate the gas turbine model can predict the performance of the actual gas turbine well.

4.2 Syngas

For the case study of syngas, a design study for a nominal 1,100 MW coal IGCC power plant was selected as the basis for calibration (Bechtel *et al.*, 2002). Four GE 7FA+e combustion turbines are used in this plant. The gas turbines produce 840 MW and the steam turbines produce 465.2 MW. The net power generation is 1154.6 MW. The GE 7FA+e gas turbine and HRSG systems have a total stack exhaust flow rate of 15,928,800 lb/hr at 238 °F. The dry syngas input to the gas turbine is 1,741,575 lb/hr. The steam injection to the gas turbine is 1,037,800 lb/hr. The performance data for a single train of a 7FA+e gas turbine combined cycle was computed based on the data provided in the report. The main inputs in the spreadsheet model are listed in Table 3.

From the design study, the heat input to the gas turbine (LHV) was reported to be $7,184 \times 10^6$ Btu/hr (Bechtel *et al.*, 2002). Therefore, the heat rate for the simple cycle of the 7FA+e gas turbine is:

$$HR_{sc} = \frac{7184 \times 10^6 \text{ Btu/hr}}{840 \text{ MW} \times 1000 \text{ kW/MW}} = 8,552 \text{ Btu/kWh}$$

Table 3. Main Input Specifications of the Combined Cycle Model based on Syngas

Description	Value
Ambient Pressure, psia	14.7
Ambient Temperature, K	288
Compressor Pressure Ratio	15.7 ^a
Combustor Pressure Drop, psia	4
Turbine Back Pressure, psia	2
Turbine Inlet Temperature, K	1600 ^a
Turbine Inlet Reference Mass Flow, lb/hr	3,612,000 ^b
Cooling Air Extraction Fraction, %	12
Adiabatic Compressor Efficiency	0.774 ^b
Adiabatic Turbine Efficiency	0.872 ^b
Shaft/Generator Efficiency	0.98
Steam Cycle Heat Rate, BTU/kWh	9,150
HRSG Outlet Temperature, °F	238 ^c
Fuel Composition, vol%	Value^c
CH ₄	0.53
CO	27.75
H ₂	19.98
CO ₂	8.59
N ₂ + Ar	1.58
H ₂ O	41.57
LHV, Btu/lb	2,831
Temperature, °F	530

^a Brooks, F.J. (2000), GER-3567H, GE Power Systems

^b Values selected based on a calibration process

^c Bechtel, et. al, (2002). The syngas composition is computed based on clean gas composition and steam injection, which is listed in Appendix.

The exhaust flow for a single train of a 7FA+e gas turbine is:

$$m_{\text{ex}} = \frac{15,928,800 \text{ lb/hr}}{4} = 3,982,200 \text{ lb/hr}$$

The power outputs for a single gas turbine combined cycle system are:

$$W_{\text{GT}} = \frac{840 \text{ MW}}{4} = 210 \text{ MW}$$

$$W_{\text{ST}} = \frac{465.2 \text{ MW}}{4} = 116.3 \text{ MW}$$

$$W_{\text{CC}} = W_{\text{GT}} + W_{\text{ST}} = 210 \text{ MW} + 116.3 \text{ MW} = 326.3 \text{ MW}$$

The efficiency of 7FA gas turbine combined cycle system is computed based on the heat input of the fuel:

$$\eta_{cc} = \frac{(840 \text{ MW} + 465.2 \text{ MW}) \times 10^3 \text{ kW/MW}}{7184 \times 10^6 \text{ Btu/hr} \times 2.93 \times 10^{-4} \text{ kWh/Btu}} \times 100\% = 62.0\%$$

The same calibration method used in the case of natural gas is applied in the case of syngas. For a GE 7FA+e gas turbine based on syngas, the estimated key measures of performance are a simple cycle LHV efficiency of 39.93%, and a power output of 210 MW. The constraint for exhaust temperature is less than 1,120 °F (Holt, 1998). For convenience, the exhaust temperature was assumed to be the same as that of natural gas, or 1,119 °F. In Figure 13, an adiabatic turbine efficiency of 0.872 and an adiabatic compressor efficiency of 0.774 were selected to obtain the desired exhaust temperature and the simple cycle efficiency, respectively. The reference mass flow at the turbine inlet was adjusted to obtain the desired power output.

To calibrate the heat rate of the steam cycle for a gas turbine combined cycle fired with syngas, the heat input to the steam cycle first needed to be estimated. As described in Section 3.0, the heat content of the steam used for syngas moisturization should be deducted from the total heat input to the HRSG since it is not available for the purpose of power production from the steam turbine. The pressure of steam used for injection in a 7FA+e gas turbine combined cycle is 400 psi (Amick *et al.*, 2002). The enthalpy of saturated steam at 400 psia is 1205.5 Btu/lb (Wark, 1983).

Another part of heat that needed to be estimated was the heat recovered from high temperature and low temperature gas cooling processes in an IGCC system. In the design study used as the calibration basis, an E-Gas (Destec) gasifier was used (Bechtel *et al.*, 2002). An E-Gas gasifier is an entrained-flow gasifier. The typical temperature of syngas out of the gasifier is 1950 °F (Buchanan, *et al.*, 1998). After gas cooling, the syngas is sent to the gas turbine at a temperature of 530 °F (Bechtel *et al.*, 2002). A significant fraction of the sensible heat in the hot gas is recovered by producing high temperature saturated steam, which is sent to the steam cycle. Thus, it can be assumed that a fraction of the sensible heat of cooling syngas from 1,950 °F to 530 °F is recovered by the steam cycle. However, the value of the fraction of heat recovery is not reported in the design study. Therefore, the selection of the fraction value is based on the model

results of a similar Texaco gasifier-based IGCC system in ASPEN Plus and the result of the steam cycle heat rate after calibration. The fraction of heat recovered from syngas cooling in the ASPEN

Table 4. Main Results and Comparison to Published Value based on Syngas

Variable	Predicted	Published Value ^a	Relative Difference
Simple Cycle Heat Rate, BTU/kWh	8,550	8,552	0
Gas Turbine Power Output, MW	210	210	0
Air Flow Rate, lb/hr	3,381,000	N/A	--
Exhaust Flow, lb/hr	4,014,700	3,982,200	0.8%
Exhaust Temp., °F	1,119	<1,120 ^c	--
Steam Turbine Power Output, MW	116.5	116.3	-0.1%
Combined Cycle Power Output, MW	326.4	326.3	0.03%
Combined Cycle Efficiency, %LHV	62.0	62.0	0

^a Bechtel Corporation, Global Energy Inc., and Nexant Inc. (2002), Contract No. DE-AC26-99FT40342, Task 1 Topical Report, IGCC Plant Cost Optimization, prepared for the U.S. Department of Energy. The outputs are converted to represent single 7FA+e gas turbine combined cycle.

^b Holt, N. (1998), 1998 Gasification Technologies Conference

model is about 0.9. The reference value of the steam cycle heat rate is generally 9,000 Btu/kWh (Buchanan *et al.*, 1998). Thus, the initial value of the heat recovery fraction was assumed to be 0.9. The total heat input into the steam cycle was estimated. To match the published combined cycle efficiency, a steam cycle heat rate of 9,150 Btu/hr was selected, which is close to 9,000 Btu/kWh. Therefore, the fraction of 0.9 was considered to be a reasonable value for estimating heat recovery from gas cooling in the steam cycle.

In Table 4, the model results after calibration are listed. The predicted values match the reference values well. The result of the combined cycle power output is very close to the published values. It also indicates that the values for the heat recovery fraction and the steam cycle heat rate are reasonable.

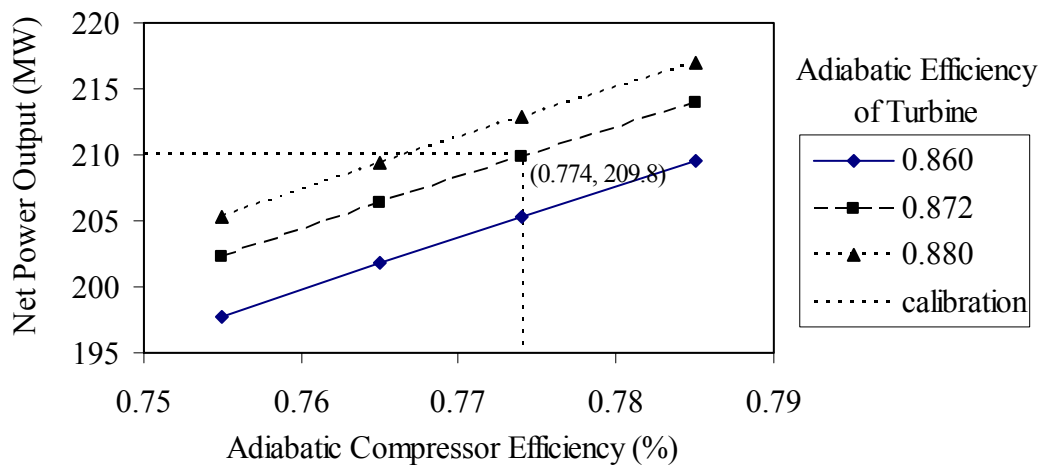
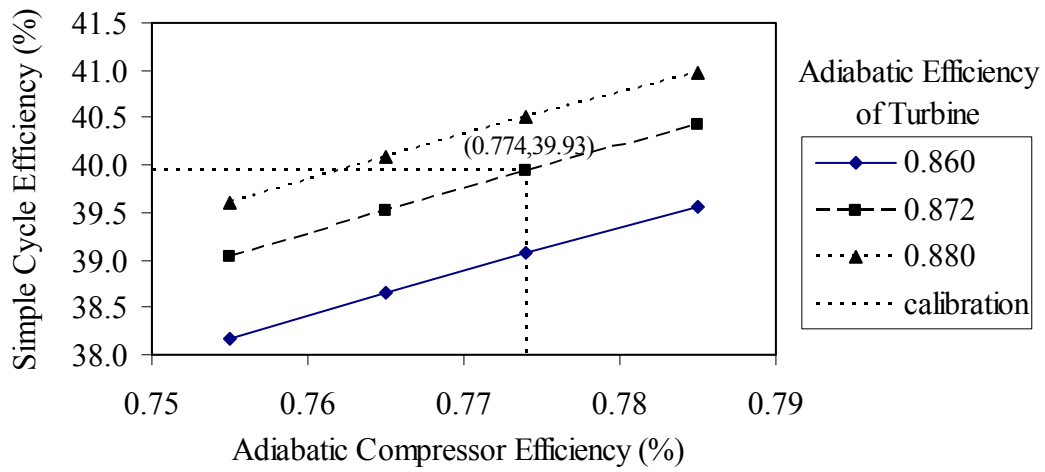
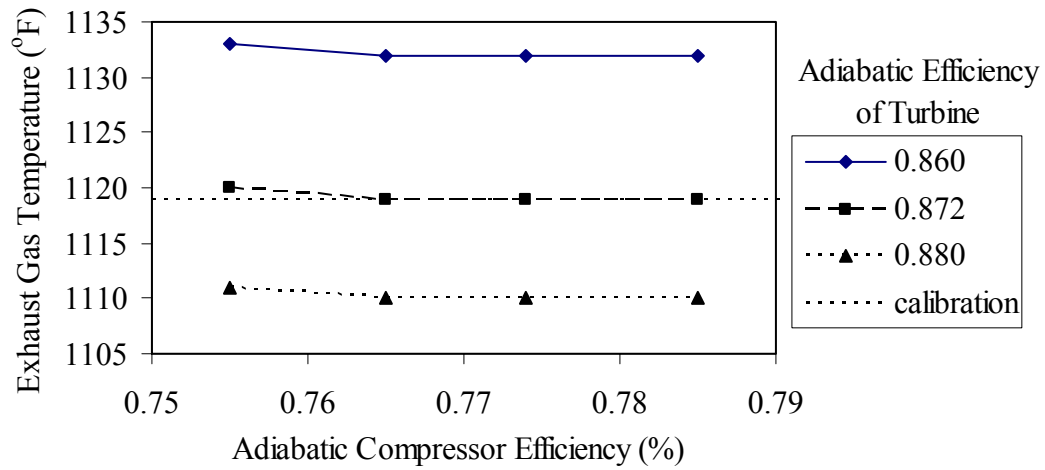


Figure 13. Calibration of the Gas Turbine Model – plots of (a) Exhaust Temperature, (b) Simple Cycle Efficiency, and (c) Simple Cycle Output versus Adiabatic Compressor Efficiency of Gas Turbine.

Note: ET = Adiabatic Turbine Efficiency of Gas Turbine

4.3 Discussion of Calibration Results

In this section, the calibration results of the gas turbine model based on natural gas and syngas are compared and discussed. The calibration results include the turbine inlet reference mass flow, adiabatic compressor efficiency, adiabatic turbine efficiency, and the steam cycle heat rate.

In the natural gas-fired gas turbine combined cycle, the turbine inlet reference mass flow is 3,159,000 lb/hr. In the syngas-fired gas turbine combined cycle, the turbine inlet reference mass flow is 3,612,000 lb/hr. The difference of turbine inlet mass flows for the two cases is due to the difference in fuel type. According to Brdar and Jones (2000), gas turbines fired on syngas have significantly larger flow rates compared to those fired on natural gas. This is due to the low heating value of syngas compared to natural gas, and to the composition of the combustion product passing through the turbine. To obtain the same turbine inlet temperature as natural gas, the flow rate of syngas is much higher than that of natural gas. Therefore, the estimated difference between the turbine inlet reference flow rate of natural gas and syngas is reasonable. The exhaust gas flow rate is mainly decided by the calibration result of the turbine reference mass flow. The results for the exhaust gas flow of the two case studies both match the related published values well. This indicates that the calibration results for turbine inlet mass flow for both fuels are reasonable.

For natural gas, the adiabatic efficiencies for the compressor and turbine are 0.9285 and 0.8485, respectively. The heat rate of the steam cycle is 8,960 Btu/kWh. For syngas, the adiabatic efficiencies for the compressor and turbine are 0.774 and 0.872, respectively, and the calibration result for the steam cycle heat rate is 9,150 Btu/kWh. Compared to the case of natural gas, there is a significant increase of the flow rate of syngas. However, the air flow to the compressor for the syngas case is 3,381,000 lb/hr, which is lower than that of the natural gas case, or 3,499,800 lb/hr. Since there is less air flowing through the compressor in the syngas case, the efficiency of the compressor for the syngas case is lower than that of natural gas. Conversely, for the syngas case, there is a larger mass flow through the turbine than for the natural gas case, which is associated with the slightly higher adiabatic efficiency for the turbine. The results of the steam cycle for both cases are very close and thus are approximately the same.

When using the gas turbine combined cycle model as part of the IECM model, the user should pay attention to the heating value of the syngas. For example, steam injection has a significant effect on the heating value of syngas. Steam injection will increase the power output of the gas turbine (Mathuousakis, 2002; Brdar and Jones, 2000). Therefore, if there are substantial differences in the moisture fraction and the heating value of syngas, the model may need to be recalibrated to obtain a reasonable power output.

Future gas turbine development mainly includes higher firing temperature, higher pressure ratio, and greater capacity. Therefore, the specifications for firing temperature, pressure ratio, and the turbine inlet mass flow should be updated and the model recalibrated for these data changes.

5.0 Cost Model

The purpose of this section is to provide estimates for the capital and annual costs for a 7FA+e gas turbine combined cycle system. At present, the detailed information about the 7F+e gas turbine for developing a cost model is still very limited and therefore, is not enough to develop a cost model. However, the cost model of a 7F gas turbine, which is in the same 7F class as 7FA+e gas turbine, has been developed and verified by Frey and Rubin (1990). Comparing the 7F and 7FA+e gas turbines, the specifications of a 7FA+e are close to that of a 7F gas turbine. The 7FA+e model features a pressure ratio of 15.7 and firing temperature of 2,420 °F. In the report by Genhardt (2000), it mentioned that the 7F model has a pressure ratio of 15.1 and a firing temperature of 2,350 °F, which are very close to the values for the 7FA+e gas turbine. Thus, the costs may not really change much among all of the various 7F alternatives since the cost for a gas turbine mainly depends on the design and capacity. Therefore, the feasibility of using this model to estimate the cost of 7FA+e gas turbine combined cycle was considered and evaluated to see if any updates should be made for accurate estimates.

There are a number of design factors that influence the cost of a gas turbine combined cycle system. For example, a syngas-fired gas turbine has higher associated costs than a natural gas-fired gas turbine because syngas requires modification of the fuel nozzles and gas manifold in the gas turbine (BGE, 1989; Buchanan, 1998). Therefore, for gas turbines fueled with natural gas and syngas,

Table 5. Total Plant Cost of NGCC with F Gas Turbine based on Difference Project Contingency Factors (2000 Dollar)

Parameters	Case 1	Case 2	Case 3
Indirect Construction Cost Factor, f_{ICC}	0.25		
Sale Tax, r_{tax}	0.06		
Engineering and home Office cost Factor, f_{EHO}	0.15		
Fixed Charge Factor, f_{fcf}	0.1034		
Variable Cost Levelization Factor, f_{vclf}	1.0000		
Process Contingency, f_{PC}	0.05		
Project Contingency, f_{PJ}	0.1	0.15	0.2
Direct Costs	Costs, 1,000\$, (2000 Dollar)		
Gas Turbine	30377	30377	30377
HRSG	10960	10960	10960
Steam Turbine	16479	16479	16479
Boiler Feedwater System	989	989	989
General Facility	8821	8821	8821
Total Direct Cost (TDC)	67627	67627	67627
Indirect Construction Costs	16907	16907	16907
Sales Tax	3348	3348	3348
Environmental Permits	1000	1000	1000
Engineering and Home Office Fee	13182	13182	13182
Total Indirect Cost (TIC)	34437	34437	34437
Process Contingency	5103	5103	5103
Project Contingency	10717	16075	21433
Total Plant Cost (TPC)	117883	123242	128600
Total Plant Cost, \$/kW	448	469	489

two different direct cost models were used. The capital and annual cost results of natural gas-fired 7FA+e gas turbine combined cycle systems were compared to the available results to verify the feasibility of the cost model. For a syngas-fired 7FA+e gas turbine, the direct costs of the combined cycle were evaluated. The annual cost for the syngas-fueled gas turbine was not available since it still needs to be integrated with other processes to form a complete IGCC system and the information cannot be provided by the performance model of a gas turbine.

5.1 Natural Gas Combined Cycle

Based on the cost model developed by Frey and Rubin (1990), the results of capital and annual costs for 7FA+e gas turbine were obtained and are listed in Table 5. In order to verify if the cost model can provide a correct estimation of the costs for a natural gas-fired 7FA+e

Table 6. Cost of Electricity of NGCC with F class gas turbine based on Case 1 with Difference Natural Gas Costs

Parameters			
Capacity Factor	0.8		
Natural Gas Cost, \$/GJ	2.78	2.88	3.32
Costs			
Inventory Capital Cost (IC), 1000\$	6841	7085	8156
Preproduction Cost (PPC), 1000\$	3472	3504	3641
Total Capital Requirement (TCR), 1000\$	129376	129651	130859
Total Capital Requirement, \$/kW	492	493	498
Fixed Operating Cost, \$(kW-yr)	9.7	9.7	9.7
Variable Operating Cost, \$(kW-yr)	18.1	18.8	21.6
Fuel Cost, mills/kWh	17.9	18.6	21.4
Incremental Variable Costs, mills/kWh	0.2	0.2	0.2
Levelized Cost of Electricity, mills/kWh	26.7	27.4	30.3

gas turbine combined cycle system, the results were compared to the related reports. Holt and Booras (2000) mentioned that the total plant cost (TPC) for a natural gas combined cycle system with an “F” gas turbine was estimated to be 505 \$/kW. Holt and Booras (2000) also mentioned that the TPC for an NGCC system with an “F” gas turbine is 410 \$/kW, as reported by Audus. The average between these two TPC’s is approximately \$450/kW. In another study (Bechtel, *et al.*, 2002), the cost of a natural gas combined cycle system with a 7FA+e gas turbine is 450\$/kW (2000 dollar). Since this is similar to the estimate reported by Holt and Booras (2000), 450\$/kW was adopted as a basis for comparison to the estimated result of the cost model.

In order to obtain the closest results to the reference data and because the project contingency in the above reference reports was not provided, the project contingency was varied from 01 to 0.2 since NGCC is a mature technology and a typical value of project contingency for preliminary estimates is 0.20 (Frey and Rubin, 1990). Other cost factors were the default values used in the NGCC cost model. The values of the other parameters concerning stream flow rates and conditions used in the computation of the direct cost for the steam cycle system were estimated and can be found in Appendix III.

From the results in Table 5, the TPC in \$/kW ranges from 448 \$/kW to 489 \$/kW. The result of Case study 1 was 448 \$/kWh, which is closest to the reference value, 450 \$/kW. Therefore, Case 1 was selected as the base case for estimating the cost of electricity. It indicated

that the project contingency of 0.1 was a suitable selection for the 7FA+e NGCC capital cost estimation.

Table 7. Comparison of Cost of NGCC with Reference Results

	Model Results (Case 1)	Reference Results	Relative Difference, %
Total Plant Cost, \$/kW	448	450	- 0.2 %
Levelized Cost of Electricity, mills/kWh	27.4	30.7	-10.7%

The annual cost results for a 7FA+e NGCC are listed in Table 6, and are based on Case 3 in Table 5 since this case is closest to the reference results. The annual cost results were also compared to the results of Holt and Booras (2000) for verification. Holt and Booras (2000) mentioned that the levelized cost of electricity for a NGCC based on a 7F gas turbine is 30.7 mills/kWh with a natural gas cost of \$2.88/GJ. Holt and Booras (2000) also cited an estimate by Audus (2000) of 22 mills/kWh based on a natural gas price of \$2/GJ. However, the result of Audus is low due to the low natural gas price. Holt and Booras (2000) mentioned that the natural gas prices of \$2.78/GJ and \$3.32/GJ were used in two other studies. Both of them were also much higher than \$2/GJ and closer to \$2.88/GJ. Therefore, the three natural gas prices were considered reasonable values and inputted into the cost model in this study.

Varying natural gas prices can provide hints for cost comparison. For example, if the same annual cost was obtained based on a lower natural gas price compared to the reference values, then it can be inferred that other factors of the costs were higher than the reference results. In Holt and Booras (2000), an 80% capacity factor was used, which was also used in this study for the purpose of comparison. The results of the levelized cost of electricity based on different natural gas costs ranged from 26.7 mills/kWh to 30.3 mills/kWh. When the natural gas price was \$3.32/GJ, the result of the cost model was very close to the reference case. However, \$3.32/GJ is higher than the natural gas price in the reference report and therefore, the cost estimation was slightly lower than the reference report.

In Table 7, the results of Case 3 are compared to the reference values. The differences between TPCs are small. The costs of electricity based on the same natural gas price of \$2.88/GJ were compared and the difference was only about 10%, which is considered to be within the precision of a budgetary cost estimate. The comparison results indicate that the cost model

developed by Frey and Rubin (1990) continues to be suitable for cost estimation of a NGCC system with a 7FA+e gas turbine without need for significant modification.

5.2 Syngas-Fueled Gas Turbine

The cost information for the syngas-fueled gas turbine combined cycle systems was collected and compared to the results of the cost model developed by Frey and Rubin (1990). The objective of this study was to determine if the direct cost for each of the main components in the present cost model should be updated according to the collected information.

The direct cost information for the power blocks of IGCC systems were collected and described for the following cases:

- Base Case: Texaco-based with 7FA Combined Cycle (Frey and Rubin, 1990);
- Case 1: Destec-based with 7FA Combined Cycle (Buchanan, *et al.*, 1998);
- Case 2: Destec-based with 501G Combined Cycle (Buchanan, *et al.*, 1998);
- Case 3: Destec-based with 7F Combined Cycle (Smith and Heaven, 1992).

The cost information for the above four cases were compared and are listed in Table 8.

In the Base Case, the direct costs for the power block of a Texaco gasifier-based IGCC plant were estimated by the cost model developed by Frey and Rubin (1990). The main components of this power block consist of a 7FA gas turbine, heat recovery steam generator (HRSG), and a steam turbine. The cost was converted to 1998 dollars. The main component costs were then individually compared to the reference reports.

For the cost of a gas turbine, the result of Case 1 was almost identical to the result of the Base Case. This is because the same gas turbine model was used in both cases and the report year of Case 1 was closer to the Base Case as compared to the other two cases. For Case 2, the cost of a gas turbine was unsuitable for comparison since the gas turbine model was W501G, which was different from the gas turbine model, GE 7FA, used in the Base Case. The result of Case 3 was slightly higher than the result of the Base Case even though the same 7F class gas turbine was used in that case. A possible explanation is that the result of Case 3 was based upon an older study and thus, might be less accurate with respect to more updated designs.

For the cost of the heat recovery steam generator (HRSG), the result of the Base Case was generally lower than the reference reports. For the cost of the steam turbine, the cost of the Base Case was a little higher than for the other cases. However, the sum of the HRSG and steam turbine costs from the Base Case,

Table 8. Direct Costs of IGCC Projects with Texaco Gasification and 7FA Combined Cycle

	Base Case	Case 1 ^a	Case 2 ^a	Case 3 ^b	Average	Difference
Description	Texaco-7FA	Destec-7FA	Destec - 501G	Destec GCC ⁱ		
Gasification	Texaco	Destec	Destec	Destec		
Plant Size	284.7	543.2	349.2	512		
Gas Turbine	7FA	7FA	501G	7F		
Cost Base (Report)	Jan. 1998	Jan. 1998	Jan. 1998	1991		
Study Year	2003	1998	1998	1992		
Case Type	Model	Conceptual	Design	Design		
Unit	Direct Capital Cost (Equipment, Material, and Labor), 10 ³ \$/kW, (Cost basis: Jan. 1998)					
Gas Turbine	124.1	122.5	--	145.6	134.1	
HRSG	43.8	62.4	54.7	52.4	56.5	
Steam Turbine	81.3	66.1	64.9	58.1	63.0	
Power Block	249.2	251.0	--	256.1	253.6	-1.7%

^a Destec based IGCC with 7FA combined cycle. DOE (1998), "Market-based Advanced Coal power Systems," Final Report, Appendix E.

^b Smith, J. and Heaven, D. (1992), "Evaluation of a 510-MWe Destec GCC Power Plant Fueled With Illinois No. 6 Coal", June. The original cost basis is 1991, which is converted to the cost base of 1998.

111\$/kWh, was much closer to the sum of the two separate parts costs in the other cases, or 111\$/kWh to 128\$/kWh. Therefore, the cost model can still provide an accurate estimate for the steam cycle costs based on the comparison results.

The individual component costs of the reference cases have been compared to the Base Case. However, the total cost for the power block has more contributions to the overall IGCC plant cost than the individual components. Therefore, the average cost values of the main components of the power block and their sum was calculated and compared to the Base Case. The relative difference between the average number and the result of the cost model was -1.7%. This difference is considered to be within the precision of a budgetary cost estimate of a power block. Although there was some difference for the individual components, the sum cost of the components or the total cost of the power block of the Base Case was close to the reference average value. Therefore, the cost model by Frey and Rubin (1990) can still be used for estimating the cost for a 7FA gas turbine combined cycle system based on syngas.

6.0 Sensitivity Analysis of Different Syngas Compositions and Inputs

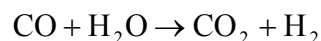
This section details the sensitivity analysis that was conducted to evaluate the effects of different syngas compositions. The purpose of this section was to determine the changes in gas turbine performance based on the gas turbine model results with different syngas composition inputs, including syngas with varying moisture and CO₂ removal fractions. Based on the changes in performance results, the effects of syngas compositions on gas turbine performance were evaluated. In addition, the changes in gas turbine performance results were compared to the relative reference values to evaluate the accuracy of the estimates of the gas turbine model.

The analysis of the effects of different syngas compositions was divided into two parts according to the source of syngas compositions. The first part of the analysis looked at the effects of different syngas compositions, due to different moisture fractions and CO₂ removal percentages, on gas turbine performance. The syngas in the calibration case was selected as a basis. Four other syngas compositions were obtained by changing the moisture fraction and amount of removed CO₂.

The second part of the analysis explored the effects of different published syngas compositions without CO₂ removal on the performance of a gas turbine. The syngas compositions were input to the gas turbine model and the main performance outputs of the gas turbine combined cycle system were compared and analyzed. Therefore, the purpose of this study was to determine how syngas composition changes affect gas turbine performance and to develop a general rule for the change of gas turbine performance due to different syngas compositions. The results from this analysis can be used to evaluate the feasibility of the gas turbine model for different syngas compositions.

6.1 Effects of Moisture Fraction and CO₂ Removal

In IGCC systems with CO₂ removal, a water-gas shift process is used to convert carbon monoxide in the syngas to carbon dioxide. The CO₂ is then removed using a separation process. The shift reaction is (Doctor *et al.*,1996):



After the CO₂ is separated, syngas rich in hydrogen is sent to the gas turbine combustor.

Table 9. Sensitivity Analysis of Different Syngas Compositions

Saturated Syngas Composition, vol%	Base Case ^a	Case 1: No CO ₂ Removal	Case 2: 85% of CO ₂ Removal	Case 3: 90% of CO ₂ Removal	Case 4: 95% CO ₂ Removal
CH ₄	0.53	0.63	0.67	0.69	0.71
CO	27.75	33.25	1.76	1.82	1.88
H ₂	19.98	23.94	58.90	60.83	62.89
CO ₂	8.59	10.29	6.66	4.59	2.37
N ₂ +Ar	1.58	1.89	2.00	2.07	2.14
H ₂ O	41.57	30	30	30	30
Total	100	100	100	100	100
Fuel LHV	2831 Btu/lb (144 Btu/scf)	3327 Btu/lb (173 Btu/scf)	6168 Btu/lb (168 Btu/scf)	6910 Btu/lb (174 Btu/scf)	7856 Btu/lb (180 Btu/scf)
Air Flow Rate, lb/hr	3,381,000	3,539,000	3,677,000	3,710,000	3,743,000
Fuel Flow Rate, lb/hr	634,000	523,100	282,400	250,800	219,600
Heat Input to Gas Turbine, 10 ⁶ Btu/hr	1,795	1,740	1,742	1,733	1,725
Exhaust Flow, lb/hr	4,015,000	4,062,000	3,959,000	3,961,000	3,962,700
Steam Injection for Moisturization, lb/hr	237,700	138,900	142,800	137,600	132,500
Exhaust Temp., °F	1,119	1,114	1,112	1,111	1,111
Gas Turbine Power Output, MW	210.0	193.1	189.5	186.5	183.6
Simple Cycle Efficiency, %LHV	39.93	37.88	37.14	36.74	36.34
Heat Input to HRSG, 10 ⁶ Btu/hr	983	967	977	975	973
Steam Turbine Power Output, MW	116.5	126.5	127.1	127.6	128.0
Combined Cycle Power Output, MW	326.4	319.6	316.6	314.1	311.7
Combined Cycle Efficiency, % LHV	62.08	62.69	62.06	61.87	61.68

^a Bechtel et al. (2002), Contract No. DE-AC26-99FT40342, Task 1 Topical Report, IGCC Plant Cost Optimization, prepared for the U.S. Department of Energy.

Four syngas compositions were selected for the sensitivity analysis. In the Base Case, the saturated syngas composition without CO₂ removal used in the calibration case (Bechtel, *et al.*, 2002) was used as the syngas composition prior to saturation or any additional treatment. For Case 1, the same dry clean syngas composition as the Base Case was used. However, it should be noted that the moisture fraction for Case 1 was 30%, while it was 41.2% in the Base Case. For Case 2 through Case 4, it was assumed that 95% CO in the same cleaned syngas was converted into CO₂ in the shift reaction. Then, three removal percentages of CO₂, 85%, 90%, and 95%,

were considered in three cases, respectively. In Case 2 through Case 4, the saturated moisture fraction was 30%. The compositions of the syngas with and without

Table 10. Effects of Fuel Heating Values on Gas Turbine Power Output

	Base Case and Case 1		Anand <i>et al.</i> (2000)	
	LHV (Btu/scf)	Gas Turbine Power Output (MW)	LHV (Btu/scf)	Gas Turbine Power Output ^a
Syngas 1	144	210	120	112%
Syngas 2	173	193.1	150	100%
Relative Difference	20%	-8%	25%	-11%

^a The gas turbine power outputs are represented as fraction with the power output of syngas 2 as basis. The relative difference is based on values of syngas 1.

different CO₂ removal were computed and are listed in Appendix III. The main outputs for the Base Case and other cases are listed in Table 9. The effects of moisture fraction, syngas with or without CO₂ removal, and different amounts of CO₂ removal on gas turbine performance are discussed in the following sections.

6.1.1 Effects of Moisture Fraction

The effects of moisture fraction were evaluated by comparing the Base Case and Case 1, since the only difference between the two syngas compositions was the moisture fraction. A greater moisture fraction in the Base Case yields a lower heating value of syngas compared to that of Case 1. The heating value of syngas had influence on the power output of the gas turbine. In Anand *et.al.* (1996), the effects of two syngases with different heating values on IGCC performance were evaluated. The two syngases were based on the same clean syngas composition, while the lower heating value syngas had more moisture than the higher heating value syngas. This situation was similar to the two syngases in the Base Case and Case 1 of this study. Therefore, the relative difference of syngas heating values and the gas turbine power outputs for the Base Case and Case 1 were compared to those found by Anand *et.al.* (1996). The small relative decrease in heating value for the Base Case and Case 1 produced a small relative change in power output when compared to the results of Anand *et.al.* (1996), which appear to be reasonable and consistent. When the moisture fraction decreased, the heating value of the syngas increased.

To reach a specific firing temperature, the requirement for syngas decreased when the energy content of syngas increased. Under the same flow rate constraint used for the first turbine nozzle, the air requirement increased when the flow rate of syngas decreased, leading to an increase in the power consumption of the compressor. Therefore, the power output of the gas

turbine decreased with increasing syngas heating value. In summary, a gas turbine fired with a higher heating value fuel will have lower power output than if it fired lower heating value fuel. This conclusion was verified by the results of the simulation. This result is also consistent with research conducted by others (Brdar and Jones, 2000; Anand, *et al.*, 1996; and Doctor *et al.*, 1996).

The difference in moisture fraction also caused a difference in the steam turbine performance. The steam turbine power output for Case 1 was higher than that of the Base Case. A lower moisture fraction means a lower amount of steam injection into the cleaned syngas and less heat deduction from the steam cycle. From the Base Case to Case 1, the decrease in the heat deduction was 119×10^6 Btu/hr, while the decrease in the heat input was only to HRSG, 16×10^6 Btu/hr. Therefore, the net energy used for power production by the steam turbine in Case 1 was 103×10^6 Btu/hr higher than the Base Case, which lead to a higher power output of the steam turbine in Case 1.

The combined cycle efficiency was decided by the total heat input to the gas turbine and the total combined cycle power output. Although the combined cycle power output of Case 1 is 2.1% lower than that of the Base Case, the total heat input of Case 1 is 3.1% lower than that of the Base Case. Thus, The combined cycle efficiency of Case 1 was higher than that of the Base Case. The reason is that the steam turbine power output in Case 1 is much higher than that of the Base Case.

In summary, the effects of moisture change caused variations in the syngas heating value. Actually, the different heating values were the direct reason for the observed differences in gas turbine performances. Another effect of moisture change was on the steam turbine performance since an alternate moisture fraction requires different steam injection from the steam cycle, which affects the net energy used for producing power in the steam cycle.

6.1.2 Effects of CO₂ Removal

Comparing Case 1 and Case 4, the difference was that the syngas without CO₂ removal was used in Case 1 while the syngas with 95% CO₂ removal was used in Case 4. The Case 4 in this study is similar to the glycol case in Doctor *et al.* (1996), which also used 95% CO₂ removal. The system in the report was a KRW Oxygen-Blown IGCC plant with two GE 7F gas turbines.

The power output of the two gas turbines was 298.8 MW in the case without CO₂ removal and it was 284.1 MW in the glycol case. The gas turbine output of the glycol case was 4.7% less than that in the case without CO₂ removal. For this study, the relative difference between the gas turbine power outputs from Case 1 and Case 4 was – 4.9%. The two different values were very close. These values indicate that the results of this study are reasonable and consistent with the result of Doctor *et al.* (1996).

For Case 1 and Case 4, it was found that the heating values on a volume basis (Btu/scf) for the two syngases were almost the same, while the heating value on a mass basis of the syngas in Case 1 was much lower than that in Case 4. The latter result is due to the unique thermodynamic features of hydrogen. In Anand, *et al.* (1996), the decrease in syngas heating value was obtained by adding moisture. Since moisture is not combustible matter, the heating values on a mass basis have the same change trend as the heating values on a volume basis. However, hydrogen is combustible and has a low heating value of 273 Btu/scf on a volume basis but a very high heating value of 51,872 Btu/lb on a mass basis (Moliere, 2002). Therefore, an increase in hydrogen composition increases the heating value of syngas on a mass basis, while the heating value on a volume basis of syngas has no significant change. The heating value on a mass basis has predominant effects on the energy performance of a gas turbine (Moliere, 2002). Therefore, the conclusion is that a gas turbine fueled with syngas having a lower heating value on a mass basis has a higher power output than a gas turbine fueled with higher heating value syngas on a mass basis.

A comparison of the results from Case 1 and Case 4 is consistent with the comparison of the results from the Base Case and Case 1. The simple cycle efficiency of Case 4 was lower than Case 1, which was due to the lower power output of the gas turbine in Case 4. The steam turbine power output in Case 4 was higher than that of Case 1, because the steam injection of Case 4 was lower than that of Case 1 and the energy input to the HRSG of Case 4 was 7×10^6 Btu/hr higher than that of Case 1. The combined cycle efficiency of Case 4 was lower than that of the Base Case due to the large decrease in gas turbine power outputs in Case 4.

When comparing Case 2 through Case 4 with different CO₂ removal percentages, the exhaust flows were almost the same for each of the three cases. The hydrogen content in the

syngas increased with increasing removal percentages, which lead to the heating values of fuel increasing both on a mass basis and volume basis. The simple cycle efficiency was related to the gas turbine power output and the heat input, which decreased with an increasing CO₂ removal fraction, due to the decrease in the power output of the gas turbine. For the steam turbine, the power output increased with increasing CO₂ removal fraction. The moisture injection decreased with decreasing syngas flow rate since the syngases have the same moisture fraction. The energy deduction due to moisture injection decreased, which lead to the steam turbine power outputs increasing from Case 2 through Case 4. The power output of the combined cycle system decreased due to the power output decrease of the gas turbine, which also lead to a slight decrease in the combined cycle efficiency with an increase in the CO₂ removal fraction.

6.2 Effects of Different Published Syngas Compositions

Several published syngas compositions were selected for analyzing the sensitive inputs and parameters of the gas turbine combined cycle model. The purpose was to further determine the effects of different syngas compositions on the gas turbine performance. The results of this section were analyzed and compared to the results of Section 6.1 to determine the general trends and effects that different syngas compositions have on gas turbine performance.

The modeling results are listed in Table 11. The same parameters were adopted as in the calibration case, which was the Base Case. The three cases from the reference reports are described as the following:

- Case 5. Sarlux: a nominal 551 MW Texaco gasifier-based IGCC fueled with Tar and co-production of hydrogen and low pressure steam. (Collodi, 2000; Brdar and Jones, 2000).
- Case 6. Texaco-IGCC: a nominal 400 MW Texaco gasifier-based IGCC plant fueled with West Kentucky Bituminous coal (Condrelli et al., 1991).
- Case 7. Destec-IGCC: a nominal 510 MW Destec gasifier-based IGCC plant fueled with Illinois No.6 coal (Smith, J. and Heaven, D., 1992).

In Table 11, from the case of Sarlux to the case of Destc-Illinois No.6 coal, the gas turbine power outputs decreased with an increase in the syngas heating value. The fuel gas flow rates also decreased. The simple cycle efficiency decreased with increasing syngas heating value.

This was due to a decreasing power output from the gas turbine that was larger than the decrease of heat input. The steam turbine power output increased due to the decrease in water fraction in the syngas. The energy deducted by moisture injection from the steam cycle decreased with increasing syngas flow rate and water fraction. The combined cycle power output had a slight decrease, yet due to a larger decrease in the heat input, the combined cycle efficiency increased. In summary, the gas turbine power output decreased and the steam turbine power output increased with increasing heating value of syngas for the typical coal syngas composition.

Comparing Table 9 and Table 11, for the typical syngas from coal gasification, the fuel heating value on a mass basis has a consistent trend with the heating value on a volume basis. However, comparing the typical coal syngas and hydrogen-rich syngas after CO₂ removal, the Table 11. Sensitivity Analysis based on Published Syngas Composition

Cases	Case 5	Case 6	Case 7
Projects	Sarlux ^a	Texaco-IGCC ^b	Destec-IGCC ^c
Sites	Italy	California	California
Date	2000	1992	1992
Gasification	Texaco	Texaco	Destec
Feedstock	Tar	West Kentucky Bituminous Coal	Illinois No. 6 Coal
Power Output	551 MW	400 MW	510 MW
Saturated Syngas Composition, vol%			
CH ₄	0.2	0.1	0.23
CO	30.6	32.3	37.16
H ₂	22.7	24.1	27.33
CO ₂	5.6	6.5	9.69
N ₂	1.1	0.7	1.31
Ar	--	0.7	0.88
H ₂ O	39.8	35.6	23.40
Total	100	100	100
Fuel LHV	3248 Btu/lb (158 Btu/scf)	3378 Btu/lb (166 Btu/scf)	3716 Btu/lb (191 Btu/scf)
Air Flow Rate, lb/hr	3,484,100	3,525,000	3,620,000
Fuel Flow Rate, lb/hr	543,700	518,100	461,100
Heat Input, 10 ⁶ Btu/hr	1,766	1,750	1,713
Exhaust Flow, lb/hr	4,027,800	4,043,000	4,062,000
Exhaust Temp., °F	1,116	1,115	1,112
Steam Injection for Moisturization, lb/hr	205,200	172,900	96,750
Gas Turbine Power Output, MW	200.3	195.6	184.8

Simple Cycle Efficiency, %LHV	38.73	38.16	36.81
Heat Input to HRSG, 10 ⁶ Btu/hr	975	971	959
Steam Turbine Power Output, MW	115.6	119.7	129.6
Combined Cycle Power Output, MW	315.9	315.3	314.4
Combined Cycle Efficiency, % LHV	61.07	61.50	62.63

^a The basic information of Sarlux is from Collodi, (2000), 2000 Gasification Technologies Conference; The syngas composition of Sarlux project are recorded in Brdar and Jones, (2000), GER-4207;

^b Condrelli, et al. (1991), EPRI IE-7365.

^c Smith and Heaven, (1992), EPRI TR-100319.

hydrogen-rich gas has a much higher fuel heating value on a mass basis than the typical coal syngas. Yet, the hydrogen-rich gas has almost the same or lower heating value on a volume basis than the typical syngas. Since the heating value on a mass basis has a significant effect on the energy performance of a gas turbine (Moliere, 2002), for a hydrogen-rich syngas, the heating value on a mass basis should be used when evaluating system performance.

When comparing syngases, another difference was the combined cycle efficiency. From Case 1 to Case 4 in Table 9, the combined cycle efficiency decreased with increasing syngas heating value, while in Table 11, the combined cycle efficiency increased with the increasing syngas heating value. An explanation for this trend is that the same moisture fraction was present for the four syngases in Case 1 to Case 4, while in Table 8, the moisture fraction decreased substantially from Case 5 to Case 7. The decrease in moisture fraction, in addition to the decrease of syngas flow rate, lead to a larger decrease in the steam injection, which in turn lead to a larger increase of the steam turbine power output in Cases 5 through 7 than in Cases 1 through 4. Thus, the combined cycle efficiency increased with increasing syngas heating value and decreasing moisture fraction.

In summary, the different heating values in syngas were caused by changes in moisture injection, different amounts of CO₂ removal, and different gasification processes. With increased moisture fraction, the heating value of syngas decreased. Increasing CO₂ removal percentage lead to an increase in the heating value of syngas on a mass basis due to the increasing hydrogen fraction. Different gasification processes in Cases 5 through 7 produced different syngas compositions and different heating values. The general rule of the effects of the syngas compositions on a gas turbine combined cycle system was determined to be that the gas turbine power output and simple cycle efficiency will decrease with increasing heating values of syngas

on a mass basis. For the combined cycle performance many other factors besides the heating value of syngas should be considered, including the moisture fractions and the different combustion products due to different syngas compositions.

From the sensitivity analysis, the gas turbine power output was not a constant value. The “210”MW used for the calibration basis was probably a generic number that was not specific to the syngases listed in Table 4. As discussed before, Anand (1996) mentioned different syngas heating values may have different gas turbine power outputs. Holt (1998) also mentioned the power output of a 7FA gas turbine may have different values other than the nominal 192 MW for different gasification processes and different coals. Therefore, the conclusions obtained from the sensitivity analysis were consistent with the results from the reference reports.

7.0 Sensitivity of Inputs

The sensitivity analysis was implemented to evaluate the effects of the changes in inputs on the main outputs of the gas turbine model. The objective of this section is to provide information about the questions: (1) what kinds of changes will be caused by the change of an input?; (2) what are the most sensitive, moderately sensitive, or least sensitive inputs of this model?. The answers to these questions were helpful to evaluate the accuracy of the estimates based on the changes of the sensitive inputs values.

The effects of inputs on three outputs were evaluated, and include gas turbine (GT) power output, simple cycle efficiency, and combined cycle efficiency. The same syngas composition used in the calibration case was selected. There were eight inputs that were evaluated based on the outputs of the gas turbine (GT) power output and simple cycle efficiency, including adiabatic turbine efficiency, adiabatic compressor efficiency, air cooling fraction, ambient temperature, ambient pressure, compressor pressure drop, turbine back pressure, and generator efficiency. The values of inputs were changed and the relative differences in the inputs compared to the corresponding values of the calibration case were computed. Only one input value was changed at a time while the others were held constant. The relative changes in the outputs were computed based on the corresponding data in the calibration case. For the combined cycle efficiency, two more inputs besides the above inputs were studied, including the

steam cycle heat rate and the HRSG outlet temperature. The effects of the input variation on the three outputs were characterized by the following diagrams in Figures 14 through 16.

In order to quantify the effects of input changes on output change, the slopes of each line in Figures 14 through 16 were determined and are listed in Table 12. A positive slope value means that the change of input caused the same trend in the outputs, while a negative slope means an opposite change occurred in the output. The results shown in Table 12 indicate a 1% increase of adiabatic turbine efficiency will cause a 1.55% increase in the gas turbine power output, a 1.55% increase in the simple cycle efficiency, and a 0.62% increase in the combined cycle efficiency.

The inputs of adiabatic turbine efficiency, adiabatic compressor efficiency, and generator efficiency had the most important effects on the three outputs. The ambient pressure was also very sensitive for the outputs of gas turbine power output and simple cycle efficiency. For the combined cycle efficiency, the steam cycle heat rate also had important effects in addition to the adiabatic efficiencies. The above inputs were identified as the most sensitive inputs, and had slopes higher than 0.35. The inputs with absolute values for slope in the range of 0.05 to 0.35 for any one output were considered to have moderate sensitivity. The moderately sensitive inputs include air cooling fraction, ambient temperature, turbine back pressure, and the HRSG outlet temperature. The input of compressor pressure drop having a slope less than 0.05 for all three outputs was identified as the least sensitive input.

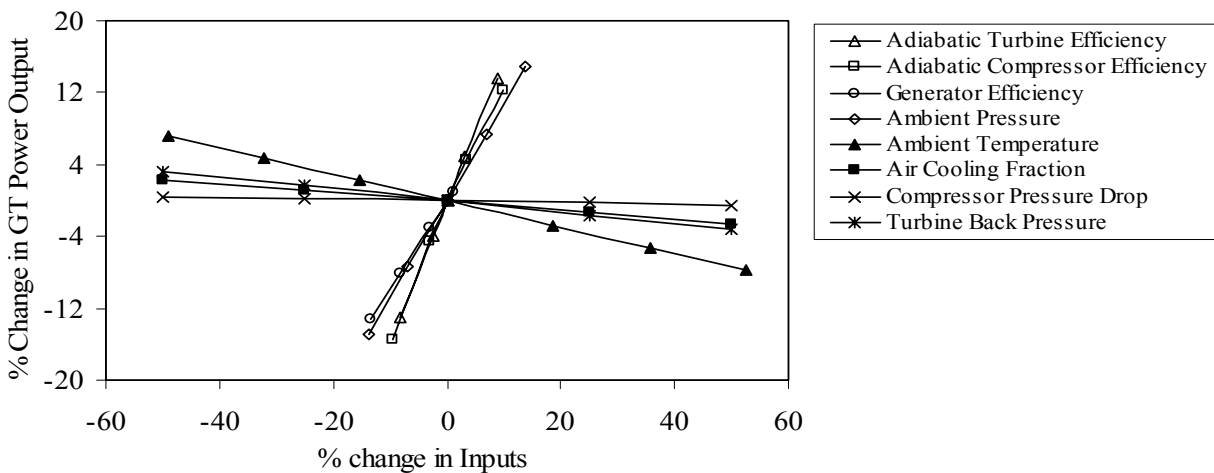


Figure 14. Changes in Inputs versus Changes in Gas Turbine (GT) Power Output

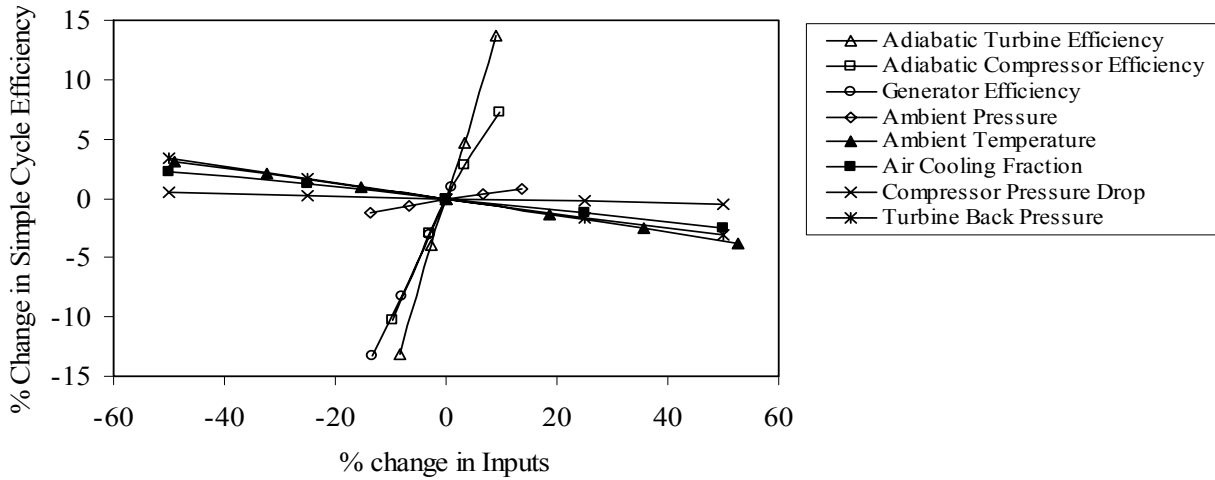


Figure 15. Changes in Inputs versus Changes in Simple Cycle Efficiency

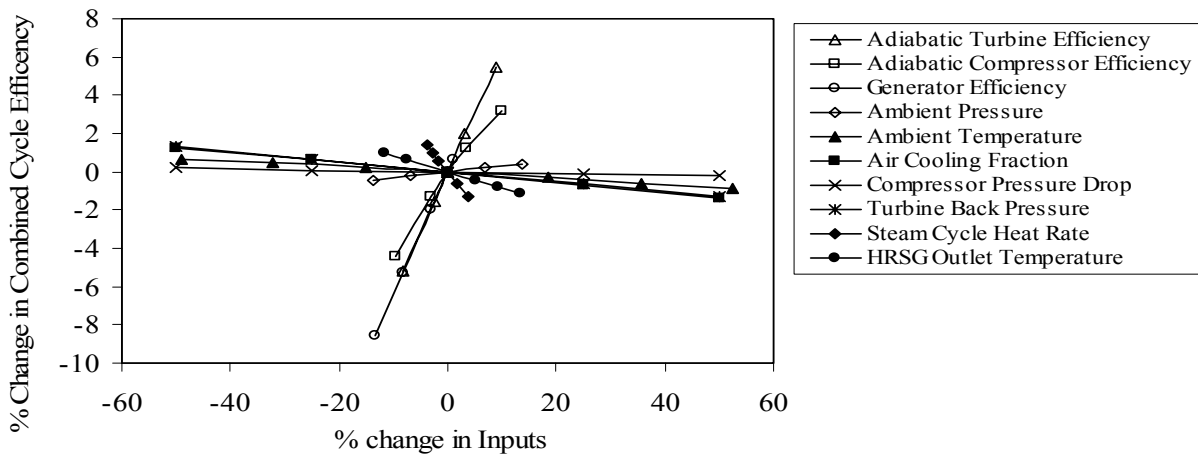


Figure 16. Changes in Inputs versus Changes in Combined Cycle Efficiency

Table 12. Slopes of Lines for Effects of Inputs Changes on Outputs

Slopes	Gas Turbine Power	Simple Cycle Efficiency	Combined Cycle Efficiency
Adiabatic Turbine Efficiency	1.55	1.55	0.62
Adiabatic Compressor Efficiency	1.43	0.90	0.39
Generator Efficiency	1.00	1.00	0.63
Ambient Pressure	1.09	0.08	0.03
Air Cooling Fraction	-0.05	-0.05	-0.03
Ambient Temperature	-0.15	-0.07	-0.02
Compressor Pressure Drop	-0.01	-0.01	-0.004
Turbine Back Pressure	-0.06	-0.06	-0.03
Steam Cycle Heat Rate			-0.36

HRSG Outlet Temperature			-0.08
-------------------------	--	--	-------

8.0 Discussion of Sensitivity Analysis

The sensitivity analysis was implemented based on different syngas compositions and different input values. Based on the sensitivity analysis, the important sensitive inputs for the gas turbine model are:

- Gas turbine specifications, including compressor pressure ratio, turbine inlet temperature, turbine inlet reference mass flow, and exhaust temperature. For a specific gas turbine, the above parameters have specific values.
- Syngas characteristics, including heating value, moisture fraction, and composition: a gas turbine fueled with high heating value syngas produces a lower power output than a gas turbine fueled with a lower heating value syngas, while the steam turbine combined with the gas turbine has a greater power output. The simple cycle efficiency decreases with increasing heating value. Based on the same clean syngas composition, the saturated syngas with less moisture will have a higher heating value. A lower moisture fraction in syngas leads to a greater power output from the steam turbine. Syngas after CO₂ removal will have more hydrogen, which leads to a higher heating value of syngas on a mass basis.
- Turbine Adiabatic Efficiency: Higher turbine adiabatic efficiency leads to lower exhaust temperature;
- Compressor Adiabatic Efficiency: Increasing the compressor adiabatic efficiency will increase the gas turbine power output and the simple cycle efficiency;
- Generator Efficiency: Higher generator efficiency will increase the gas turbine power output and the efficiencies of the simple cycle and combined cycle systems;
- Ambient Pressure: Higher ambient pressure will produce higher compressor outlet pressure under a constant pressure ratio. Thus, the turbine inlet pressure will

increase, which leads to greater power output from the turbine and thus, higher gas turbine power output;

- Steam cycle heat rate: Lower steam cycle heat rate leads to higher steam turbine power output.

It is important to have the correct values of the above inputs for an accurate estimation of gas turbine performance.

Based on the sensitivity analysis, the inputs of moderate sensitivity include:

- Ambient temperature;
- Combustor pressure drop;
- Turbine back pressure;
- Air cooling fraction;
- HRSG outlet temperature.

The input of compressor pressure ratio was identified as the lower sensitivity input in the gas turbine model.

In summary, the gas turbine model developed in this study can accurately estimate the performance and cost of a 7F gas turbine and its combined cycle system. The effects of the syngas compositions and the controlled effects of changes in inputs on outputs were investigated. The results indicate that this model can be used to reasonably estimate the performance of a gas turbine fired with different syngas compositions. The sensitivities of the inputs were identified by the relative changes in outputs caused by the relative changes in inputs. This relationship gives insight into the important effective factors for estimating the gas turbine performance, as it answered the questions about what kinds of change will be caused by the change of an input.

9.0 Conclusions

In this study, a performance model for simple and combined cycle gas turbine systems was developed and calibrated. The mass and energy balance of a simple cycle and combined cycle gas turbine model was implemented and the multiple stages of the compressor and turbine and cooling air splits were simulated. The use of the combined cycle model was demonstrated considering the two cases of natural gas and syngas. In the combined cycle case study based on syngas, the heat from gas cooling recovered in the steam cycle and the heat deduction due to steam or water injection to the syngas were estimated. The gas turbine model was calibrated based on natural gas and syngas for a typical “Frame 7F” heavy duty gas turbine. The turbine inlet reference mass flow, adiabatic turbine efficiency, adiabatic compressor efficiency, and the steam cycle heat rate were calibrated to obtain the desired outputs. The calibrations for the cases of natural gas and syngas were compared and discussed. The calibration results indicate that the gas turbine can predict the performance of the gas turbine well for model outputs that were not used as a design basis for the calibration.

The main inputs to the model that can be specified by a user include fuel composition (including carbon monoxide, hydrogen, methane, carbon dioxide, water vapor, and nitrogen), pressure ratio, firing temperature, reference mass flow at the turbine inlet, ambient pressure, ambient temperature, combustor pressure drop, turbine backpressure, adiabatic compressor and turbine efficiencies, combined cycle heat rate, cooling air splits, steam cycle heat rate, generator efficiency, and exhaust outlet temperature. The main outputs of the model include simple cycle heat rate, gas turbine power output, air flow, exhaust flow, exhaust temperature, steam turbine power output, and combined cycle efficiency. For combined cycle systems implemented in an IGCC system, the user can also specify heat duties associated with syngas cooling and the effect of steam or water injection into the syngas with respect to the steam cycle energy balance.

The cost model was combined with the gas turbine performance model. The estimated results were compared with other reference values. The capital and annual cost for the natural gas combined cycle system and the direct cost for a syngas-fueled gas turbine were estimated. The cost models demonstrate that the modeling results of both the natural gas fueled turbine or the syngas-fueled gas turbine were consistent with the reference values.

The results of sensitivity analysis indicated that this model can be used to estimate the performance of a gas turbine fired with different syngas compositions. The sensitivity analysis of the inputs gives insight into the important effective factors for estimating gas turbine performance. This research provides guidelines to judge the accuracy of estimates from the gas turbine model by considering the expected change in the outputs caused by the relative change of the inputs. This project demonstrates that an accurate and sensitive model can be implemented in a spreadsheet, which makes the model much easier to utilize. In addition, implementation into a spreadsheet makes this model more accessible than the model in ASPEN Plus since one does not have to be trained in the use of ASPEN. Thus, this study supports the ability to do desktop simulations, which in turn supports policy analysis.

10.0 Nomenclature

English Letter Symbols

DC	=	Direct Cost, \$
e_a	=	The fraction of excess air
GT	=	Gas Turbine
$h_{c,out,isentropic}$	=	Enthalpy of air at the outlet of an isentropic compressor, J/gmole
$h_{i,j}$	=	Enthalpy at device i, where j = in or out, J/gmole
$h_i(T)$	=	Enthalpy of species i at temperature T (Rankin), Btu/lbmole syngas
$H_{air,stoic}$	=	Enthalpy of air needed in a stoichiometric reaction with fuel, J/gmole
H_{fuel}	=	Fuel Enthalpy, J/gmole
$H_{product,stoic}$	=	Enthalpy of stoichiometric reaction product, J/gmole
HR	=	Heat rate of the steam cycle, Btu/kWh
LHV	=	Lower heating value of fuel, Btu/lb
$m_{C,i,air}$	=	Air flow rate to the stage i of compressor, lb/hr
$m_{Comb,air}$	=	Air flow rate to the combustor, lb/hr
$m_{Comb,ex}$	=	Exhaust flow rate out of the combustor, lb/hr
m_{fuel}	=	Fuel mass flow rate, lb/hr
$m_{T,i}$	=	Stream flow rate to the stage i of turbine, lb/hr
$m_{T,out}$	=	Stream flow rate at the outlet of turbine, lb/hr
M_{fuel}	=	Fuel molar flow rate, lbmole/hr
MW_{fuel}	=	Molar weight of fuel, lb/lbmole
MW_{air}	=	Molecular weight of air, lb/lbmole
$N_{T,GT}$	=	Total number of gas turbines
P_a	=	Ambient pressure of inlet air
$P_{C,i,out}$	=	Pressure at the outlet of stage i of compressor, where i = 1, 2, or 3
$P_{T,i,out}$	=	Pressure at the outlet of stage i of turbine, where i = 1, 2, or 3
$P_{i,j}$	=	Pressure at device i, where j = in or out
Q_{fuel}	=	Total energy input of the system, Btu/hr
Q_H	=	Energy input of HRSG, Btu/hr
Q_S	=	Shaft work, Btu/hr
r_p	=	Pressure ratio of compressor outlet pressure to compressor inlet pressure

$r_{p,i}$	=	Pressure ratio of a single stage i of compressor
$r_{p,turb}$	=	Pressure ratio of turbine inlet pressure to turbine outlet pressure
$r_{p,turb,i}$	=	Pressure ratio of a single stage i of turbine
$s_{i,j}$	=	Specific Entropy at device i , where j = in or out
T_a	=	Ambient temperature of inlet air
$T_{T,in}$	=	Turbine inlet temperature
W_{CC}	=	Net power output of the combined cycle, MW
W_{SC}	=	Net power output the simple cycle, MW
W_{ST}	=	Net electricity produced by the steam turbine, MW
y_i	=	Mole fraction of compound i

Greek Letter Symbols

Δh_i	=	Total enthalpy difference between the inlet and outlet of device i
$\Delta h_{r,i}$	=	Enthalpy of reaction for compound i (j/gmole)
Δp_{back}	=	turbine back pressure (psi)
η_C	=	Adiabatic compressor efficiency
η_S	=	Shaft work efficiency
η_T	=	Adiabatic turbine efficiency
η_{CC}	=	Combined cycle efficiency
η_{SC}	=	Simple cycle efficiency

Subscript

act	=	Actual
air	=	Air
C	=	Compressor
CC	=	Combined Cycle
Comb	=	Combustor
ex	=	Exhaust gas
fuel	=	Fuel
H	=	Heat Recovery Steam Generator
In	=	Inlet

NGCC	=	Natural Gas Combined Cycle
IGCC	=	Integrated Gasification Combined Cycle
Out	=	Outlet
ref	=	Reference
s	=	Stage
SC	=	Simple Cycle
SG	=	Syngas
ST	=	Steam Turbine
T	=	Turbine

Species

CO	=	Carbon Monoxide
CO ₂	=	Carbon Dioxide
CH ₄	=	Methane
H ₂ O	=	Water
N ₂	=	Nitrogen
O ₂	=	Oxygen

11.0 References

Amick, P., Herbanek, R., and Jones, R.M. (2002), "NO_x Control for IGCC Facilities Steam vs. Nitrogen," 2002 Gasification Technologies Conference, San Francisco, CA, October 27-30.

Anand, A.K., Cook, C.S., Corman, J.C., and Smith, A.R.(1996), "New Technology Trends for Improved IGCC System Performance, Journal of Engineering for Gas Turbines and Power, vol. 118: 732-736.

Anderson, F.E. (1993), "Generator Cooling, Air or Hydrogen?" GER-3738B, the 37th GE Turbine State-of-the-Art Technology Seminar, GE Power Generation, Schenectady, NY, July 1993.

Audus, H. (2000), "Leading Options for the Capture of CO₂ at Power Stations," IEA Greenhouse Gas R&D Program. Presented at the Fifth International Conference on Greenhouse Gas Control (GHGT-5), Cairns, Queensland, Australia. August 14-16.

Bechtel Corporation, Global Energy Inc., and Nexant Inc. (2002), "Gasification Plant Cost and Performance Optimization (Contract No. DE-AC26-99FT40342), Task 1 Topical Report, IGCC Plant Cost Optimization," Prepared for the U.S. Department of Energy, National Energy Technology Laboratory, Washington DC, May 2002.

Berkenpas, M.B., H.C. Frey, J.J. Fry, J. Kalagnanam, and E.S. Rubin, "Integrated Environmental Control Model: Technical Documentation," Prepared by Carnegie Mellon University for U.S. Department of Energy, Pittsburgh, PA. May 1999.

BGE (1989), "Baltimore Gas and Electric Company's Study of a Shell-Based GCC Power Plant," EPRI GS-6283. Prepared by Baltimore Gas and Electric Company for Electric Power Research Institute, Palo Alto, CA. March 1989.

Brdar, R.D. and Jones, R.M. (2000), "GE IGCC Technology and Experience with Advanced Gas Turbines," GE Power Systems, Schenectady, NY.

Brooks, F.J. (2000), "GE Gas Turbine Performance Characteristics," GER-3567H, GE Power Systems, Schenectady, NY.

Buchanan, T.L., DeLallo, M.R., Goldstein, H.N., Grubbs, G.W., and Whites, J.S. (1998), "Market-based Advanced Coal Power Systems," Prepared for the U.S. Department of Energy, Office of Fossil Energy, Washington DC, December 1998.

Collodi, G. (2000), "Operation of ISAB Energy and Sarlux IGCC Projects," the 2000 Gasification Technologies Conference, San Francisco, California, October 8-11, 2000.

Condorelli, P., Smelser, S.C., and McCleary, G. J. (1991), "Engineering and Economic Evaluation of CO₂ Removal From Fossil-Fuel-Fired Power Plants, Volume 2: Coal Gasification-Combined-Cycle Power Plant," prepared by FLUOR DANIEL, Inc. for Internal Energy Agency, Paris, France, and EPRI, Palo Alto, California, June.

Doctor, R.D., Molburg, J.C., and Thimmapuram, P.R., (1996), "KRW Oxygen-Blown Gasification Combined Cycle: Carbon Dioxide Recovery, Transport, and Disposal," Energy Systems Division, Argonne National Laboratory, U.S. Department of Energy, August.

Frey, H.C., and N. Akunuri (2001), "Probabilistic Modeling and Evaluation of the Performance, Emissions, and Cost of Texaco Gasifier-Based Integrated Gasification Combined Cycle Systems Using ASPEN," Prepared by North Carolina State University for Carnegie Mellon University and U.S. Department of Energy, Pittsburgh, PA, January 2001

Frey, H.C. and Rubin, E.S. (1990), "Stochastic Modeling of Coal Gasification Combined Cycle Systems: Cost Models for Selected Integrated Gasification Combined Cycle (IGCC) Systems," Prepared for U.S. Department of Energy, Office of Fossil Energy, Morgantown Energy Technology Center, Morgantown, West Virginia, June.

Frey, H.C. and Rubin, E.S. (1991), "Development and Application of a Probabilistic Evaluation Method for Advanced Process Technologies," DOE/MC 24248-3105, Prepared by Carnegie Mellon University for U.S. Department of Energy, Morgantown, WV, April

Gebhardt, E. (2000), "The F Technology Experience Story," GE Power Systems, Atlanta, GA.

Holt, N. (1998), "IGCC Power Plants – EPRI Design & Cost Studies," Presented at 1998 EPRI/GTC Gasification Technologies Conference, San Francisco, CA, October 6, 1998.

Holt, N. and Booras, G. (2000), "Analysis of Innovative Fossil Fuel Cycles Incorporating CO₂ Removal," 2000 Gasification Technologies Conference, San Francisco, CA. October 8-11.

Hornick, M. J. and McDaniel, J. E. (2002), "Tampa Electric Polk Power Station Integrated Gasification Combined Cycle Project," Final Technical Report, Prepared for the U. S. Department of Energy, Office of Fossil Energy, National Energy Technology Laboratory (NETL), Morgantown, West Virginia, August.

Jones, R.M., Wolff, J., and GmbH U., (2002), "Reducing CO₂ Emission by Hydrogen IGCC Power Plants," GE Power System, 2002 Gasification Technologies Conference, San Francisco, CA, October 27-30.

Mathioudakis, K. (2002), "Analysis of the Effects of Water Injection on the Performance of a Gas Turbine," *Journal of Engineering for Gas Turbines and Power* 2002 (124): 489 – 495.

Matta, R.K., Mercer, G.D. and Tuthill, R.S. (2000), "Power Systems for the 21st Century – "H" Gas Turbine Combined-Cycles," GE Power Systems, Schenectady, NY.

Matta, R.K., Mercer, G.D. and Tuthill, R.S. (2000), "Power Systems for the 21st Century – "H" Gas Turbine Combined-Cycles," GE Power Systems, Schenectady, NY.

Moliere, M. (2002), "Benefit from the Wide Fuel Capability of Gas Turbines: a Review of Application Opportunities," GT-2002-30017, Proceedings of ASME TURBO EXPO 2002, June 3-6, 2002, Amsterdam, The Netherlands.

Rubin, E.S., J.S. Salmento, J.G. Barrett, C.N. Bloyd, and H.C. Frey (1986), *Modeling and Assessment of Advanced Processes for Integrated Environmental Control of Coal-Fired Power Plants*, NTIS DE86014713, Prepared by Carnegie-Mellon University for the U.S. Department of Energy, Pittsburgh, Pennsylvania, July 1986.

Rubin, E.S., J.S. Salmento, and H.C. Frey (1988), "Cost-Effective Emission Controls for Coal-Fired Power Plants," *Chemical Engineering Communications*, 74:155-167 (1988).

Rubin, E.S., J.S. Salmento, H.C. Frey, A. Abu-Baker, and M. Berkenpas, *Modeling of Integrated Environmental Control Systems for Coal-Fired Power Plants*, Final Report, DOE Contract No. DE-AC22-87PC79864, Prepared by Carnegie-Mellon University for the U.S. Department of Energy, Pittsburgh, Pennsylvania, April 1991, 214p.

Rubin, E.S., J.R. Kalagnanam, H.C. Frey, and M.B. Berkenpas (1997), "Integrated Environmental Control Concepts for Coal-Fired Power Plants," *Journal of the Air and Waste Management Association*, 47(11):1180-1188 (November 1997)

Smith, J. and Heaven, D. (1992), "Evaluation of a 510-MWe Destec GCC Power Plant Fueled with Illinois No. 6 Coal," Prepared by FLUOR DANIEL, INC., prepared for EPRI, Palo Alto, California, June.

Wark, K. (1983). *Thermodynamics*, Fourth Edition. McGraw-Hill Book Company: New York.

Appendix I. IECM Enthalpy Functions

$$h_{\text{N}_2}(T) = 6.66 T + 2.8333 \times 10^{-4} T^2 - 3655.83 \quad (\text{I-1})$$

$$h_{\text{O}_2}(T) = 7.16 T + 2.7778 \times 10^{-4} T^2 + 129600 T^{-1} - 4164.05 \quad (\text{I-2})$$

$$h_{\text{CO}_2}(T) = 10.55 T + 6 \times 10^{-4} T^2 + 660960 T^{-1} - 7066.27 \quad (\text{I-3})$$

$$h_{\text{H}_2\text{O}}(T) = 7.17 T + 7.1111 \times 10^{-4} T^2 - 25920 T^{-1} - 4004.44 \quad (\text{I-4})$$

$$h_{\text{CH}_4}(T) = 2.975 T + 5.0914 \times 10^{-3} T^2 + 4.427 \times 10^{-7} T^3 - 112100 T^{-1} - 2785.67 \quad (\text{I-5})$$

$$h_{\text{CO}}(T) = 6.79 T + 2.7222 \times 10^{-4} T^2 + 35640 T^{-1} - 3788.8 \quad (\text{I-6})$$

$$h_{\text{H}_2}(T) = 6.52 T + 2.1667 \times 10^{-4} T^2 - 38880 T^{-1} - 3489.04 \quad (\text{I-7})$$

where the enthalpy is in units of BTU/lbmole and the temperature is in units of degrees Rankine.

Appendix II. Clean Syngas and Saturated Syngas Composition of the Nominal 1,100 MW IGCC Plant

Table II-1. Composition of Clean Syngas and Saturated Syngas ^a

Fuel Composition, vol%	Cleaned Syngas	Saturated Syngas
CH ₄	0.9	0.53
CO	47.5	27.75
H ₂	34.2	19.98
CO ₂	14.7	8.59
N ₂	1.5	0.88
Ar	1.2	0.70
H ₂ O	0	41.57
Total	100	100
Syngas Mass Flow, lb/hr	1,741,575	
Steam Injection, lb/hr	1,037,800	

^a Bechtel *et al.* (2002), Contract No. DE-AC26-99FT40342, Task 1 Topical Report, IGCC Plant Cost Optimization, prepared for the U.S. Department of Energy. The outputs are converted to represent single 7FA+e gas turbine combined cycle.

The molar weight for cleaned syngas is 21.5076. Therefore, the molar flow rate of cleaned syngas is:

$$M_{\text{cleansyn}} = \frac{1,741,575 \text{ lb/hr}}{21.5076 \text{ lb/lbmol}} = 80974.9 \text{ lbmol/hr}$$

The steam injection molar flow rate is:

$$M_{\text{steam}} = \frac{1,037,800 \text{ lb/hr}}{18.015 \text{ lb/lbmol}} = 57607.5 \text{ lbmol/hr}$$

Therefore, the moisture fraction in the saturated syngas is:

$$y_{\text{H}_2\text{O}} = \frac{57607.5 \text{ lbmol/hr}}{80974.9 \text{ lbmol/hr} + 57607.5 \text{ lbmol/hr}} \times 100\% = 41.57\%$$

Other compositions of the saturated syngas are calculated based on the moisture fraction and the cleaned syngas composition.

Appendix III. Inputs of Stream Flow Rates and Conditions for Cost Model

In order to use the cost model to calculate the cost of the natural gas combined cycle system with a Frame 7F gas turbine, the flow rate of raw water, polished water, cooling water, and the flow rate and pressure of high pressure steam need to be estimated as inputs for the cost model.

First, the flow rate and pressure of the high steam are estimated. The steam cycle condition in the gas turbine combined cycle model is 1450 psia/1000 °F/1000 °F. In Condrelli *et al.*(1992), the pressure for the high pressure steam is 1465 psia and the temperature is 1000 °F for a 1450 psi/1000 °F/1000 °F steam cycle with F gas turbine. The total energy input to the steam cycle has been estimated in Eq.(89) of section 3.0. Condrelli *et al.* (1992) did not give the information about the percentage of heat in the total energy input to the steam cycle used in high pressure steam generating. Based on another report from DOE (1998), in two NGCC cases, there are 68% and 82% of the total heat input used for producing high pressure steam. The average value is 75%. Therefore, it is assumed that 75% of the total heat input is used to generate high pressure steam. The enthalpy for the superheated steam of 1465psia/1000 °F is 1491 Btu/lb (Singer, 1981). Therefore, the mass flow of the high pressure steam is estimated as:

$$m_{\text{hps,HR}} = \frac{Q_{\text{H,NGCC}} \times 0.75}{h_{\text{hps,HR}}} \quad (\text{III-1})$$

where,

$m_{\text{hps,HR}}$ = the mass flow of high pressure steam in steam cycle, lb/hr;

$h_{\text{hps,HR}}$ = the enthalpy of the high pressure steam. It is 1491 Btu/lb for the 1465psia/1000 °F steam in this study.

Based on the steam balance in Condrelli *et al.* (1992), the high steam is 66% of the total steam turbine condensate. In NGCC, the makeup water consists of seal water and boiler blowdown water, while in the steam cycle in IGCC, the makeup water also includes the water used in coal slurry and saturation of syngas. The case in Condrelli *et al.* (1992) is a combined cycle in IGCC plant. Therefore, the makeup water used for coal slurry and saturation of syngas is

not accounted for the estimation of raw water used in NGCC. Then the makeup water or raw water is 2% of the total condensate. The raw water flow rate is estimated as:

$$m_{rw} = \frac{m_{hps,HR}}{0.66} \times 0.02 \quad (\text{III-2})$$

where,

m_{rw} = the raw water flow rate, lb/hr.

The polished water is the sum of the raw water and the steam cycle condensate:

$$m_{pw} = m_{rw} + \frac{m_{hps,HR}}{0.66} \quad (\text{III-3})$$

where,

m_{pw} = the polished water flow rate, lb/hr.

The cooling water requirement is estimated based on the equation in Frey and Rubin (1990):

$$m_{cw} = 9.3763 \times W_{CC} - 273.8 \quad (\text{III-4})$$

where,

m_{cw} = the cooling water flow rate, gal/min;

W_{cc} = the net power output of the natural gas combined cycle, MW.

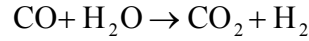
Appendix IV. Syngas Composition after Different CO₂ Removal Degree

Table IV-1. Composition of Cleaned Syngas and Syngas after CO₂ Removal

Syngas Composition, vol%	Cleaned Syngas ^a	Cleaned Syngas with 95% CO conversion to CO ₂	85% of CO ₂ Removal	90% of CO ₂ Removal	95% CO ₂ Removal
CH ₄	0.9	0.62	0.95	0.99	1.02
CO	47.5	1.64	2.52	2.60	2.69
H ₂	34.2	54.66	84.14	86.90	89.84
CO ₂	14.7	41.22	9.52	6.55	3.39
N ₂	1.5	1.03	1.59	1.64	1.70
Ar	1.2	0.83	1.27	1.31	1.36
H ₂ O	0	0	0	0	0
Total	100	100	100	100	100

^a Bechtel Corporation, Global Energy Inc., and Nexant Inc. (2002), Contract No. DE-AC26-99FT40342, Task 1 Topical Report, IGCC Plant Cost Optimization, prepared for the U.S. Department of Energy. The outputs are converted to represent single 7FA+e gas turbine combined cycle.

The shift reaction is (Doctor *et al.*, 1996):



After 95% CO conversion to CO₂, the molar flow rate of syngas increase and the composition of syngas is:

$$y'_{\text{CO}} = \frac{y_{\text{CO}} \times (1 - f_{\text{conv}})}{1 + f_{\text{conv}} y_{\text{CO}}}$$

$$y'_{\text{CO}_2} = \frac{y_{\text{CO}_2} + f_{\text{conv}} y_{\text{CO}}}{1 + f_{\text{conv}} y_{\text{CO}}}$$

$$y'_{\text{H}_2} = \frac{y_{\text{H}_2} + f_{\text{conv}} y_{\text{CO}}}{1 + f_{\text{conv}} y_{\text{CO}}}$$

$$y'_i = \frac{y_i}{1 + f_{\text{conv}} y_{\text{CO}}}$$

where,

$$f_{\text{conv}} = 0.95;$$

i = CH₄, CO, N₂ and Ar.

For different CO₂ removal fraction, the composition of syngas after CO₂ removal is:

$$y_i'' = \frac{y_i'}{1 - f_{\text{removal}} y'_{\text{CO}_2}}$$
$$y_{\text{CO}_2}'' = \frac{y'_{\text{CO}_2} \times (1 - f_{\text{removal}})}{1 - f_{\text{removal}} y'_{\text{CO}_2}}$$

where,

$f_{\text{removal}} = 0.85, 0.9, \text{ or } 0.95;$

$i = \text{CH}_4, \text{CO}, \text{H}_2, \text{N}_2 \text{ and Ar.}$